

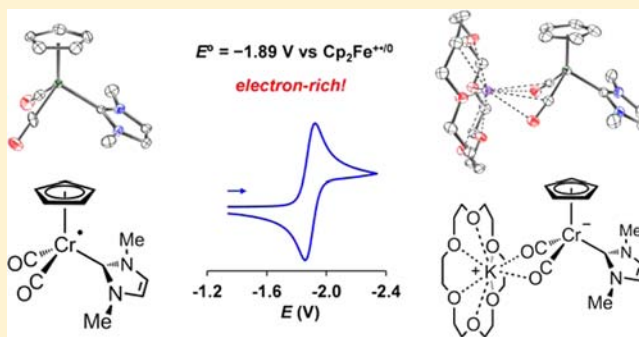
Structural and Spectroscopic Characterization of 17- and 18-Electron Piano-Stool Complexes of Chromium. Thermochemical Analyses of Weak Cr–H Bonds

Edwin F. van der Eide,[†] Monte L. Helm,[†] Eric D. Walter,[‡] and R. Morris Bullock^{*,†}

[†]Chemical and Materials Sciences Division and [‡]Environmental and Molecular Sciences Laboratory, Pacific Northwest National Laboratory, P.O. Box 999, Richland, Washington 99352, United States

Supporting Information

ABSTRACT: The 17-electron radical $\text{CpCr}(\text{CO})_2(\text{IME})^\bullet$ (IME = 1,3-dimethylimidazol-2-ylidene) was synthesized by the reaction of IME with $[\text{CpCr}(\text{CO})_3]_2$, and characterized by single crystal X-ray diffraction and by electron paramagnetic resonance (EPR), IR, and variable temperature ^1H NMR spectroscopy. The metal-centered radical is monomeric under all conditions and exhibits Curie paramagnetic behavior in solution. An electrochemically reversible reduction to 18-electron $\text{CpCr}(\text{CO})_2(\text{IME})^-$ takes place at $E_{1/2} = -1.89(1)$ V vs $\text{Cp}_2\text{Fe}^{+/0}$ in MeCN, and was accomplished chemically with K_8 in tetrahydrofuran (THF). The salts $\text{K}^+[(18\text{-crown-6})[\text{CpCr}(\text{CO})_2(\text{IME})]^{-1/2}\text{THF}]$ and $\text{K}^+[\text{CpCr}(\text{CO})_2(\text{IME})]^{-3/4}\text{THF}$ were crystallographically characterized. Monomeric ion pairs are found in the former, whereas the latter has a polymeric structure because of a network of $\text{K}\cdots\text{O}(\text{CO})$ interactions. Protonation of $\text{K}^+[(18\text{-crown-6})[\text{CpCr}(\text{CO})_2(\text{IME})]^{-1/2}\text{THF}]$ gives the hydride $\text{CpCr}(\text{CO})_2(\text{IME})\text{H}$, which could not be isolated, but was characterized in solution; a $\text{p}K_a$ of 27.2(4) was determined in MeCN. A thermochemical analysis provides the Cr–H bond dissociation free energy (BDFE) for $\text{CpCr}(\text{CO})_2(\text{IME})\text{H}$ in MeCN solution as 47.3(6) kcal mol⁻¹. This value is exceptionally low for a transition metal hydride, and implies that the reaction $2[\text{Cr}\text{--}\text{H}] \rightarrow 2[\text{Cr}^\bullet] + \text{H}_2$ is exergonic ($\Delta G = -9.0(8)$ kcal mol⁻¹). This analysis explains the experimental observation that generated solutions of the hydride produce $\text{CpCr}(\text{CO})_2(\text{IME})^\bullet$ (typically on the time scale of days). By contrast, $\text{CpCr}(\text{CO})_2(\text{PCy}_3)\text{H}$ has a higher Cr–H BDFE (52.9(4) kcal mol⁻¹), is more stable with respect to H_2 loss, and is isolable.



INTRODUCTION

Metal-centered 17-electron radicals have received much attention for several decades.¹ Such radicals are usually very reactive. Typical reactivity patterns are dimerization,² binding of a donor ligand to form 19-electron adducts³ (of importance to substitution⁴ and disproportionation⁵ reactions), and halogen atom abstraction² from halogenated hydrocarbons.

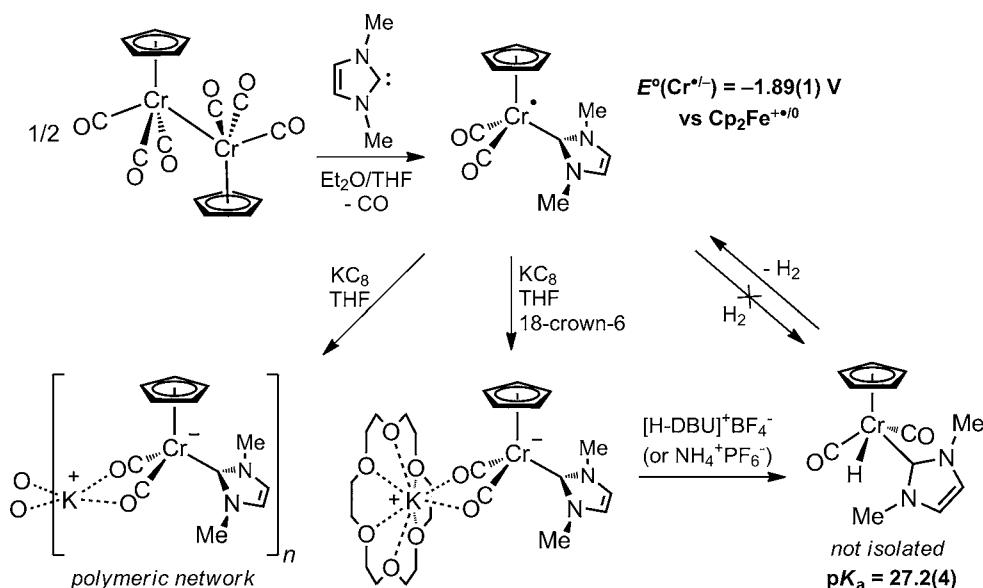
Metal-centered radicals have also been observed⁶ to abstract hydrogen atoms from hydrocarbons to give 18-electron hydrides; the reverse reaction, hydrogen atom transfer from transition metal hydrides to hydrocarbyl radicals, has been studied⁷ in detail. Hydrogen atom transfer to and from organic compounds, mediated by transition metal hydrides and radicals, have found application in chain transfer processes in radical polymerizations and in reductive cyclization reactions.^{8,9} In this regard, determination of the thermodynamic properties of M–H bonds, either calorimetrically or using thermochemical cycles, is of interest. In 18-electron metal hydrides, M–H homolytic bond dissociation enthalpies (BDEs) as high as 82 kcal mol⁻¹ ($\text{CpOs}(\text{CO})_2\text{H}$)⁶ and as low as 55 kcal mol⁻¹ ($\text{HV}(\text{CO})_4(\text{Ph}_2\text{P}(\text{CH}_2)_4\text{PPh}_2)$)⁹ have been measured.

We have recently shown that N-heterocyclic carbenes (NHCs) significantly stabilize 17-electron tungsten radicals $\text{CpW}(\text{CO})_2(\text{L})^\bullet$.^{10–12} In accordance with the increased stability of $\text{CpW}(\text{CO})_2(\text{NHC})^\bullet$ with respect to the parent $\text{CpW}(\text{CO})_3^\bullet$, the W–H bonds in $\text{CpW}(\text{CO})_2(\text{NHC})\text{H}$ were found^{11,12} to be 5–8 kcal mol⁻¹ weaker than in $\text{CpW}(\text{CO})_3\text{H}$. Because chromium hydrides generally have weaker M–H bonds than tungsten hydrides (e.g.: BDE = 62 kcal mol⁻¹ for $\text{CpCr}(\text{CO})_3\text{H}$ ^{13,14} vs 73 kcal mol⁻¹ for $\text{CpW}(\text{CO})_3\text{H}$ ¹³), we reasoned that $\text{CpCr}(\text{CO})_2(\text{NHC})\text{H}$ should have a particularly weak Cr–H bond. Here we report a structural, electrochemical, and spectroscopic study of the 17-electron radical $\text{CpCr}(\text{CO})_2(\text{IME})^\bullet$ (IME = 1,3-dimethylimidazol-2-ylidene) and the electron-rich anion $\text{CpCr}(\text{CO})_2(\text{IME})^-$ and the hydride $\text{CpCr}(\text{CO})_2(\text{IME})\text{H}$ derived from it. An analogous series of tricyclohexylphosphine complexes is also described. We show that $\text{CpCr}(\text{CO})_2(\text{IME})\text{H}$ (which is not isolable in pure form) has a Cr–H bond that is 9 kcal mol⁻¹ weaker than in the parent $\text{CpCr}(\text{CO})_3\text{H}$, and even weaker than that of $\text{HV}(\text{CO})_4(\text{Ph}_2\text{P}$

Received: November 9, 2012

Published: January 23, 2013

Scheme 1



$(\text{CH}_2)_4\text{PPh}_2$),⁹ whereas Cr–H bond weakening is less dramatic in $\text{CpCr}(\text{CO})_2(\text{PCy}_3)\text{H}$.

RESULTS

Synthesis and Structure of $\text{CpCr}(\text{CO})_2(\text{IMe})^{\bullet}$. $\text{CpCr}(\text{CO})_2(\text{IMe})^{\bullet}$ was synthesized (Scheme 1) by the addition of a freshly generated THF/ Et_2O solution of 1,3-dimethylimidazol-2-ylidene¹⁵ (IMe) to a dark green suspension of $[\text{CpCr}(\text{CO})_3]_2$ in Et_2O at 20 °C, resulting in the evolution of a gas (presumably CO) and a color change from dark green to light orange. Precipitation of the product by addition of hexane, followed by sublimation at <1 mTorr at 100–110 °C, afforded analytically pure $\text{CpCr}(\text{CO})_2(\text{IMe})^{\bullet}$ in 80% yield as an amorphous, dull orange-brown powder.

Orange single crystals of $\text{CpCr}(\text{CO})_2(\text{IMe})^{\bullet}$ were grown by diffusion of hexane into a fluorobenzene solution, and were analyzed by X-ray diffraction. The complex crystallizes in the centrosymmetric space group $P\bar{1}$, and the asymmetric unit contains four crystallographically independent molecules. Since the independent molecules have nearly identical metrical parameters (see below and in the Supporting Information, Table S1), only one molecule is displayed in Figure 1. The shortest separation between any pair of chromium atoms is 6.3952(14) Å, confirming the monomeric nature of the radicals. In the nearly C_s -symmetric molecules, the carbene orientation is such that the approximate mirror plane bisects the carbene ligand. We quantify this orientation using the parameter θ , which we previously¹² defined as the absolute value of the dihedral angle between the planes $\text{Cp}_{\text{centroid}}\text{--Cr--C}_{\text{(carbene)}}$ and $\text{Cr--C}_{\text{(carbene)--(N)}_2$. For the molecule shown in Figure 1, θ is 89.6°, and it falls in the range 85–88° for the other three molecules. The three legs of the piano-stool geometry are irregularly positioned around Cr: the $\text{C}_{\text{(CO)}}\text{--Cr--C}_{\text{(CO)}}$ angle of 78.2(3)° is significantly smaller than the $\text{C}_{\text{(carbene)}}\text{--Cr--C}_{\text{(CO)}}$ angles of 96.6(3) and 95.7(3)°. (In the four independent molecules, angles $\text{C}_{\text{(CO)}}\text{--Cr--C}_{\text{(CO)}}$ span the range 76.1(3) to 78.6(3)°, and the angles $\text{C}_{\text{(carbene)}}\text{--Cr--C}_{\text{(CO)}}$ span the range 95.1(3) to 100.6(3)°.)

Spectroscopic and Electrochemical Characterization of $\text{CpCr}(\text{CO})_2(\text{IMe})^{\bullet}$. $\text{CpCr}(\text{CO})_2(\text{IMe})^{\bullet}$ is sparingly soluble

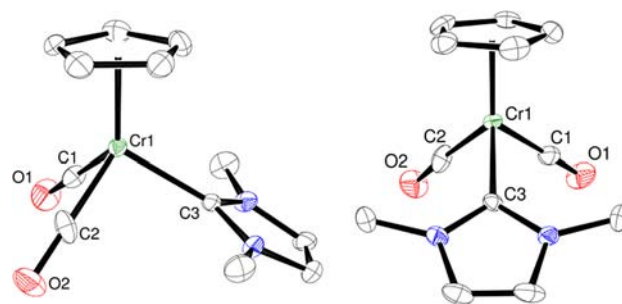


Figure 1. Two views of one of the four crystallographically independent molecules of $\text{CpCr}(\text{CO})_2(\text{IMe})^{\bullet}$ (50% probability ellipsoids, hydrogens omitted). Selected bond lengths (Å): Cr1– $\text{Cp}_{\text{centroid}}$, 1.873(3); Cr1–C3, 2.053(6); Cr1–C1, 1.822(6); Cr1–C2, 1.804(6); C1–O1, 1.166(7); C2–O2, 1.192(8). Selected bond angles (deg): C1–Cr1–C2, 78.2(3); C1–Cr1–C3, 96.6(3); C2–Cr1–C3, 95.7(3).

in hexane, but dissolves readily in aromatic and in polar solvents, giving yellow, air-sensitive solutions.¹⁶ The IR spectrum in tetrahydrofuran (THF) (Table 1) shows carbonyl stretching bands ($\tilde{\nu}_{\text{CO}}$) at 1899 and 1778 cm^{-1} . Two bands are always observed, regardless of the solvent or the concentration. We also recorded the near-infrared (NIR) spectrum, based on Atwood and Geiger's observation¹⁷ that 17-electron piano-stool complexes undergo low-energy electronic transitions involving the singly occupied molecular orbital (SOMO). As shown in Figure 2, $\text{CpCr}(\text{CO})_2(\text{IMe})^{\bullet}$ displays a weak absorption at $\lambda_{\text{max}} = 1455 \text{ nm}$.

The ^1H NMR spectrum of $\text{CpCr}(\text{CO})_2(\text{IMe})^{\bullet}$ displays paramagnetically broadened and shifted resonances. In toluene- d_8 (500 MHz, 295 K) these are found at 30.7 ($\approx 2\text{H}$, $\Delta\nu_{1/2} \approx 4500 \text{ Hz}$), 12.9 ($\approx 5\text{H}$, $\Delta\nu_{1/2} = 690 \text{ Hz}$) and 3.1 ppm ($\approx 6\text{H}$, $\Delta\nu_{1/2} = 240 \text{ Hz}$); similar shifts and linewidths are observed in CD_3CN solvent. The temperature dependence of the observed ^1H chemical shifts (δ_{obs}) was investigated in toluene- d_8 over the temperature range –30 to +70 °C (Figure 3). Equation 1 shows the expected temperature dependence of δ_{obs} for a Curie paramagnet, which $\text{CpCr}(\text{CO})_2(\text{IMe})^{\bullet}$ obeys. The term $C_{\text{M}}T^{-1}$ is the hyperfine shift, and δ_{dia} is the (hypothetical) diamagnetic

Table 1. IR Data^a ($\tilde{\nu}_{\text{CO}}$, in cm^{-1})

entry	complex	MeCN		THF	
1	$\text{CpCr}(\text{CO})_2(\text{Ime})^\bullet$	1893	1767	1899	1778
2	$\text{CpCr}(\text{CO})_2(\text{PCy}_3)^\bullet$	1902	1777	1909	1787
3	$\text{K}^+[\text{CpCr}(\text{CO})_2(\text{Ime})]^{-3/4}\text{THF}$	1737	1655	1725	1644
4	$\text{K}^+(18\text{-crown-6})[\text{CpCr}(\text{CO})_2(\text{Ime})]^{-1/2}\text{THF}$	1737	1656	1739	1653
5	$\text{K}^+(18\text{-crown-6})[\text{CpCr}(\text{CO})_2(\text{PCy}_3)]^-$	1762	1681	1767	1681
6	$\text{CpCr}(\text{CO})_2(\text{Ime})\text{H}$	1900	1810	1904	1819
7	$\text{CpCr}(\text{CO})_2(\text{PCy}_3)\text{H}$	1910	1841	1917	1851
8	$[\text{CpCr}(\text{CO})_2(\text{Ime})(\text{MeCN})]^+[\text{B}(\text{C}_6\text{F}_5)_4]^-$	1977	1908		
9	$[\text{CpCr}(\text{CO})_2(\text{PCy}_3)(\text{MeCN})]^+[\text{B}(\text{C}_6\text{F}_5)_4]^-$	1980	1908		

^aSpectra are provided in the Supporting Information

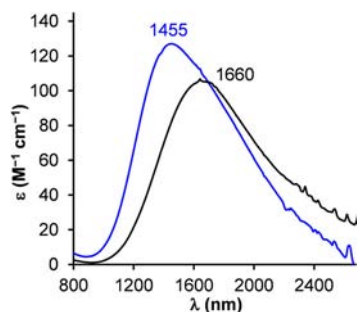


Figure 2. NIR spectra of $\text{CpCr}(\text{CO})_2(\text{Ime})^\bullet$ (blue trace) and $\text{CpCr}(\text{CO})_2(\text{PCy}_3)^\bullet$ (black trace), recorded in hexafluorobenzene.

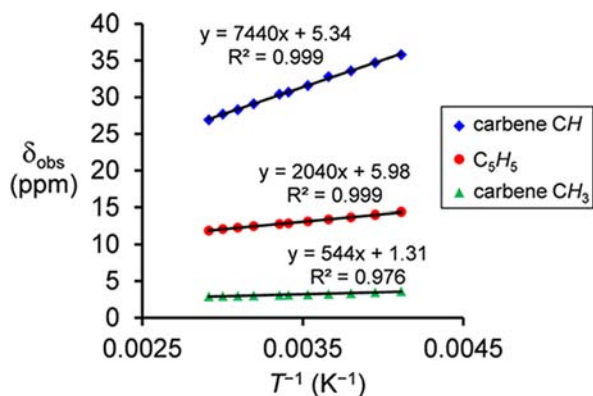


Figure 3. Temperature dependence of the observed ^1H chemical shifts of $\text{CpCr}(\text{CO})_2(\text{Ime})^\bullet$ (500 MHz, toluene- d_8) from -30 to $+70$ $^\circ\text{C}$.

shift obtained at $T^{-1} = 0$. The electron–proton coupling constants (A_{H} , in Hz) can be obtained from the slopes C_{M} by the relationship in Equation 2,¹⁸ which gives $A_{\text{H}} = 0.94$, 0.26 , and 0.07 MHz for the carbene CH, Cp, and carbene CH_3 protons, respectively. Additionally, y -intercepts of $5.3(3)$, $6.0(1)$, and $1.3(1)$ ppm are realistic diamagnetic shifts expected for these types of protons.

$$\delta_{\text{obs}} = C_{\text{M}}T^{-1} + \delta_{\text{dia}} \quad (1)$$

$$A_{\text{H}} = C_{\text{M}} \frac{3\gamma_{\text{H}}k_{\text{B}}}{2\pi g_{\text{e}}\mu_{\text{B}}S(S+1)} \quad (2)$$

Electron paramagnetic resonance (EPR) spectra of $\text{CpCr}(\text{CO})_2(\text{Ime})^\bullet$ were recorded at 9.4 GHz in toluene, in both the fluid and the frozen state (Figure 4). Hyperfine coupling (A) to ^{53}Cr ($I = 3/2$, 9.6% natural abundance) is observed in both spectra, but coupling to ^1H nuclei is not observed, which is in

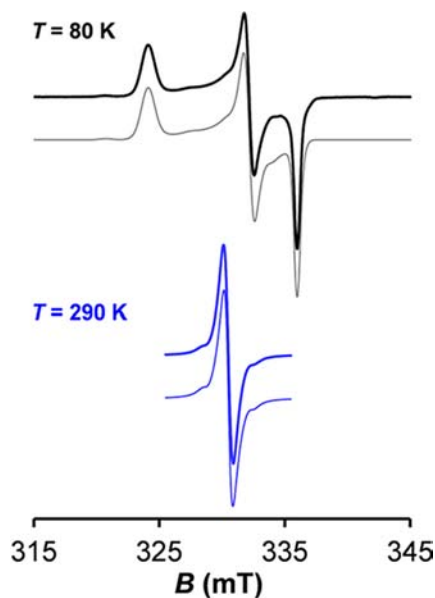


Figure 4. EPR ($\nu = 9.4$ GHz) spectra of $\text{CpCr}(\text{CO})_2(\text{Ime})^\bullet$ in toluene. The lower lines in each pair are obtained by simulation (290 K: $g_{\text{iso}} = 2.028$, $A_{\text{iso}}(^{53}\text{Cr}) = 35$ MHz; 80 K: $g_1 = 2.068$, $g_2 = 2.018$, $g_3 = 1.995$, $A_1(^{53}\text{Cr}) = 65$ MHz, $A_2(^{53}\text{Cr}) = 30$ MHz, $A_3(^{53}\text{Cr}) = 10$ MHz). See Supporting Information for simulation details.

agreement with the small (<1 MHz) A_{H} determined by ^1H NMR spectroscopy. The spectra were simulated for a low spin ($S = 1/2$) system; the employed spin-Hamiltonian parameters are provided in the caption of Figure 4.

Cyclic voltammetry of $\text{CpCr}(\text{CO})_2(\text{Ime})^\bullet$ in MeCN reveals an electrochemically reversible ($i_{\text{a}}/i_{\text{c}} \approx 0.97$ at $\nu = 0.1$ V s^{-1} , Figure 5) reduction at $E_{1/2} = -1.89(1)$ V vs $\text{Cp}_2\text{Fe}^{+/0}$, with a 65 mV peak-to-peak separation (cf. 66 mV for $\text{Cp}_2\text{Co}^{+/0}$ when cobaltocene is added as a reference); we assign this wave to the couple $\text{CpCr}(\text{CO})_2(\text{Ime})^{\bullet/-}$. A quasi-reversible ($i_{\text{c}}/i_{\text{a}} \approx 0.66$ at $\nu = 0.1$ V s^{-1}) oxidation with a peak-to-peak separation of 95 mV occurs at $E_{1/2} = -0.61(1)$ V vs $\text{Cp}_2\text{Fe}^{+/0}$. The cathodic wave is broader than the anodic wave, and broadens further as the scan rate is increased. Since separate experiments (see below) show that the acetonitrile adduct $\text{CpCr}(\text{CO})_2(\text{Ime})(\text{MeCN})^+$ is produced upon oxidation, the quasi-reversible process is assigned to the couple $\text{CpCr}(\text{CO})_2(\text{Ime})(\text{MeCN})^+/\text{CpCr}(\text{CO})_2(\text{Ime})^\bullet$.

Reactivity of $\text{CpCr}(\text{CO})_2(\text{Ime})^\bullet$. We treated $\text{CpCr}(\text{CO})_2(\text{Ime})^\bullet$ with 1000 psi H_2 in CD_3CN in a polyether ether ketone (PEEK) NMR tube,¹⁹ and recorded ^1H NMR spectra at 1 h intervals, to check for the possible formation of

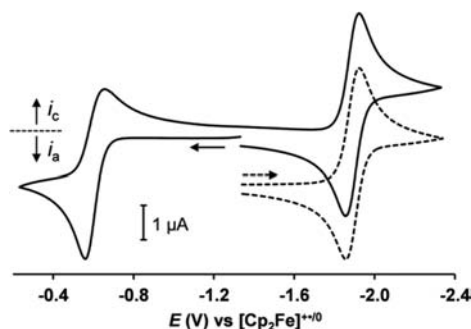


Figure 5. Background-corrected cyclic voltammograms of $\text{CpCr}(\text{CO})_2(\text{IMe})^\bullet$ ($\nu = 0.1 \text{ V s}^{-1}$, $0.1 \text{ M } ^t\text{Bu}_4\text{N}^+\text{PF}_6^-$ in MeCN). Horizontal arrows indicate initial scan directions (no Faradaic current passing at the start of the scan). The dotted voltammogram is vertically offset for clarity.

18-electron hydride $\text{CpCr}(\text{CO})_2(\text{IMe})\text{H}$ (Scheme 1). However, no observable amounts of the hydride formed even after 16 h. (We have generated $\text{CpCr}(\text{CO})_2(\text{IMe})\text{H}$ in solution by protonation of $\text{CpCr}(\text{CO})_2(\text{IMe})^-$, as described in a later section.) Further, treatment of $\text{CpCr}(\text{CO})_2(\text{IMe})^\bullet$ with the radical trap²⁰ 2,6-di-*tert*-butyl-1,4-benzoquinone did not result in adduct formation, as the IR spectrum remained unchanged. In contrast, we found¹² earlier that the tungsten radical $\text{CpW}(\text{CO})_2(\text{IMe})^\bullet$ does form a stable adduct.

Chemical redox reactions proceeded in accordance with the electrochemical observations. Oxidation of $\text{CpCr}(\text{CO})_2(\text{IMe})^\bullet$ with $\text{Ph}_3\text{C}^+\text{B}(\text{C}_6\text{F}_5)_4^-$ ($E^\circ(\text{Ph}_3\text{C}^+) \approx -0.1 \text{ V vs Cp}_2\text{Fe}^{+/0}$)²¹ in MeCN generated a species with increased $\bar{\nu}_{\text{CO}}$ values (Table 1), which we assign to the cation *cis*- $\text{CpCr}(\text{CO})_2(\text{IMe})(\text{MeCN})^+$. Coordination of MeCN is crucial for the stabilization of the cation; complete decomposition took place within 5 min when the oxidation of $\text{CpCr}(\text{CO})_2(\text{IMe})^\bullet$ was performed in fluorobenzene. Even in neat MeCN, the stability of the cation is rather limited; it stays intact for short periods of time (minutes), but complete decomposition of *cis*- $\text{CpCr}(\text{CO})_2(\text{IMe})(\text{MeCN})^+$ occurs within an hour. We have not undertaken further efforts to isolate it. On the other hand, reduction of $\text{CpCr}(\text{CO})_2(\text{IMe})^\bullet$ with KC_8 in THF proceeded smoothly and cleanly to give an orange solution of $\text{K}^+[\text{CpCr}(\text{CO})_2(\text{IMe})]^-$ (Scheme 1). This ion pair was thoroughly characterized, as described below.

Structures of $\text{K}^+(18\text{-crown-6})[\text{CpCr}(\text{CO})_2(\text{IMe})]^-$ and $\text{K}^+[\text{CpCr}(\text{CO})_2(\text{IMe})]^-$. Addition of 18-crown-6 to a filtered THF solution of $\text{K}^+[\text{CpCr}(\text{CO})_2(\text{IMe})]^-$ and subsequent precipitation with hexane gave $\text{K}^+(18\text{-crown-6})[\text{CpCr}(\text{CO})_2(\text{IMe})]^- \cdot 1/2 \text{ THF}$ as fine, orange needles in 87% yield. Single crystals were grown from a supersaturated THF solution at room temperature, giving orange blocks suitable for X-ray diffraction. The complex crystallizes in the non-centrosymmetric space group *Pca*2₁, with two crystallographically independent contact ion pairs and one THF molecule per asymmetric unit. In both ion pairs (Figure 6), all of the six crown oxygens bind to the potassium cation. The range of $\text{K} \cdots \text{O}_{(\text{crown})}$ distances is 2.83–3.10 Å (average: 2.94 Å) for K1, and 2.83–3.00 Å (average: 2.91 Å) for K2, and the potassiums are displaced significantly (0.90 Å for K1; 0.84 Å for K2) away from the mean planes formed by the crown oxygens, toward the carbonyls on the Cr. Whereas both Cr1-bound carbonyls further interact²² with K1, only one Cr2-bound carbonyl undergoes such an interaction with K2 (see also Table 2).

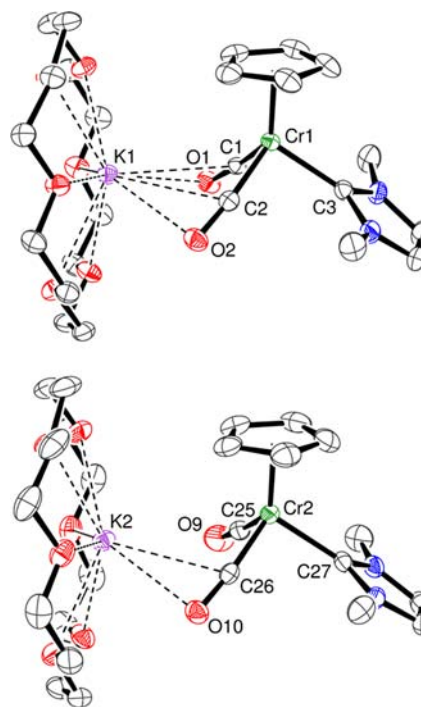


Figure 6. Two crystallographically independent molecules of $\text{K}^+(18\text{-crown-6})[\text{CpCr}(\text{CO})_2(\text{IMe})]^- \cdot 1/2 \text{ THF}$ (50% probability ellipsoids; hydrogens and THF solvent omitted). Selected metrical data are provided in Table 2.

We have also determined the crystal structure of $\text{K}^+[\text{CpCr}(\text{CO})_2(\text{IMe})]^-$ in the absence of the crown ether. A saturated THF solution of $\text{K}^+[\text{CpCr}(\text{CO})_2(\text{IMe})]^-$ (no 18-crown-6 added), allowed to concentrate slowly over several weeks, deposited several orange single crystals. Analysis by X-ray diffraction showed them to be of composition $\text{K}^+[\text{CpCr}(\text{CO})_2(\text{IMe})]^- \cdot 3/4 \text{ THF}$, crystallized in the space group *P*2₁, with an asymmetric unit containing four formula units of $\text{K}^+[\text{CpCr}(\text{CO})_2(\text{IMe})]^-$ and three molecules of THF. Two THF molecules are simply solvents of crystallization, and the remaining tetrameric conglomerate $\{\text{K}^+[\text{CpCr}(\text{CO})_2(\text{IMe})]^- \}_4(\text{THF})$ is the building block for somewhat flattened pillars that run parallel to the crystallographic *a* axis (Figure 7 and Supporting Information, Figure S1). Cyclopentadienide, carbene, and potassium-coordinating THF ligands form the periphery of the pillars, while the carbonyl ligands point toward the centrally located potassium cations, forming a network of $\text{K} \cdots \text{O}_{(\text{CO})}$ interactions. Nineteen unique $\text{K} \cdots \text{O}_{(\text{CO})}$ interactions occur (average $d(\text{K} \cdots \text{O}_{(\text{CO})}) = 2.77 \text{ \AA}$; range = 2.59–2.97 Å); only one in four potassium cations is terminally ligated by a THF ($d(\text{K} \cdots \text{O}) = 2.745(2) \text{ \AA}$). Parameters pertaining to these and other interactions are tabulated in detail in the Supporting Information.

The four individual anionic Cr fragments, together with the nearest potassium cations, are displayed in Figure 8. In addition to the $\text{K} \cdots \text{O}$ interactions, the carbene ligands on Cr1 and Cr2 interact with K1 and K3 in κ^1 and η^3 fashions, respectively ($\text{K1} \cdots \text{N2}$, 3.301(3); $\text{K3} \cdots \text{N3}$, 3.276(3); $\text{K3} \cdots \text{N4}$, 3.339(3); $\text{K3} \cdots \text{C15}$, 3.073(3) Å). Whereas both carbonyls on Cr3 and Cr4 pinch a potassium cation (K4 and K1, respectively), there is no such pinching for the Cr1 and Cr2 carbonyls.

NMR Characterization of $\text{K}^+(18\text{-crown-6})[\text{CpCr}(\text{CO})_2(\text{IMe})]^- \cdot 1/2 \text{ THF}$. Generation and Characterization of $\text{CpCr}(\text{CO})_2(\text{IMe})\text{H}$. The ¹H NMR spectrum of $\text{K}^+(18\text{-$

Table 2. Selected Bond Lengths (Å) and (Dihedral) Angles (deg) for the $K^+[CpCr(CO)_2(Ime)]^-$ Salts

	$K(18\text{-crown-6})^+$ $[CpCr(CO)_2(Ime)]^{-1/2}THF$		$K^+[CpCr(CO)_2(Ime)]^{-3/4}THF$			
	Cr1	Cr2	Cr1	Cr2	Cr3	Cr4
Cr–Cp _{centroid}	1.863(1)	1.867(1)	1.862(2)	1.862(2)	1.871(2)	1.876(2)
Cr–C _(carbene)	2.045(2)	2.049(2)	2.036(3)	2.055(3)	2.032(3)	2.045(3)
Cr–C _{(CO)^a}	1.779(2), 1.777(-2)	1.778(2), 1.779(2)	1.784(3), 1.757(-3)	1.768(3), 1.777(-3)	1.772(3), 1.776(-3)	1.774(3), 1.774(-3)
C–O ^a	1.195(2), 1.197(-2)	1.200(2), 1.209(2)	1.201(4), 1.227(-4)	1.216(4), 1.202(-4)	1.203(4), 1.207(-4)	1.198(4), 1.205(-4)
K \cdots O _{(CO)^a}	3.003(1), 2.971(-1)	3.859(2) ^b , 2.852(1)	2.80 ^c	2.78 ^c	2.78 ^c	2.73 ^c
K \cdots O _(crown or THF)	2.94 ^d	2.91 ^d		2.745(2)		
C _(CO) –Cr–C _(CO)	81.86(7)	89.41(8)	92.23(14)	91.76(15)	84.06(14)	86.75(14)
θ	84.7	87.1	73.9	80.5	88.6	83.5

^aWhen two values are given, the first value applies to the CO ligand with the lowest label number (see Figures 6 and 8). ^bNot considered a significant K \cdots O interaction. ^cAverage of six, five, or four values (see Figure 8); average of all 19 values is 2.77 Å. ^dAverage of six values.

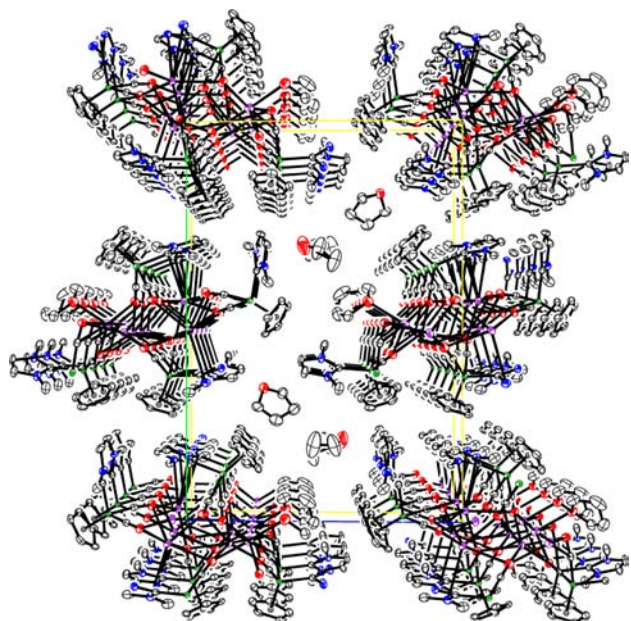


Figure 7. Perspective view of the crystal structure of $K^+[CpCr(CO)_2(Ime)]^{-3/4}THF$ along the crystallographic a axis.

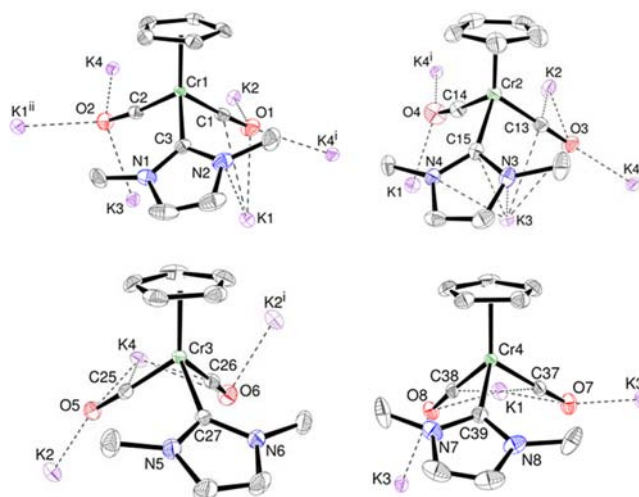


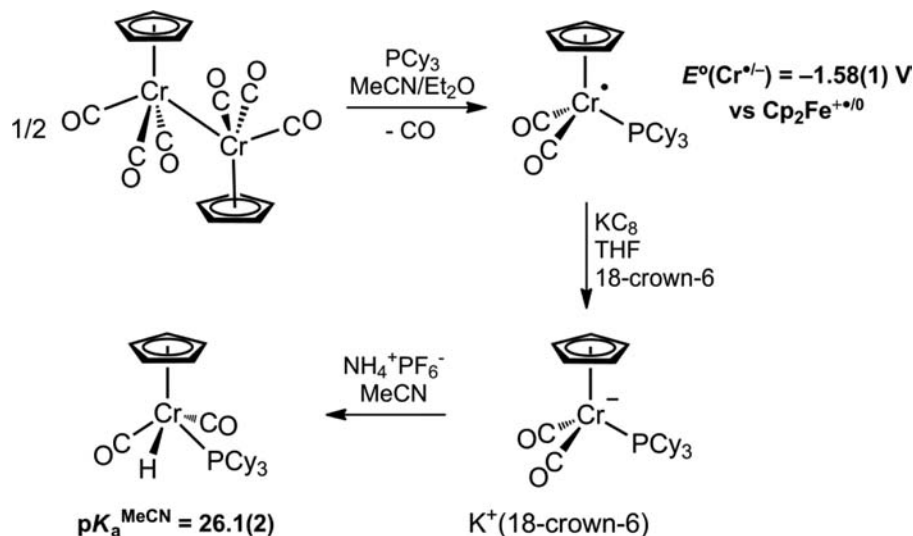
Figure 8. Structures of the four $CpCr(CO)_2(Ime)^-$ fragments and the nearest K^+ ions (50% probability ellipsoids; hydrogens omitted) in $K^+[CpCr(CO)_2(Ime)]^{-3/4}THF$. Atoms labeled with superscript 'i' or 'ii' are related to their nonsuperscripted counterparts by unit translation along the crystallographic a axis. Selected metrical data are provided in Table 2.

crown-6)[$CpCr(CO)_2(Ime)]^{-1/2}THF$ in CD_3CN displays broad resonances at 7.0 ($\approx 2H$, $\Delta\nu_{1/2} = 200$ Hz), 4.09 ($\approx 5H$, $\Delta\nu_{1/2} = 35$ Hz), and 3.86 ppm ($\approx 6H$, $\Delta\nu_{1/2} = 7$ Hz) for the protons belonging to the anion. The addition²³ of about 1 mg of KC_8 resulted in a drastic sharpening and slight shifting of these signals, now appearing as singlets at 6.84 (2H), 4.00 (5H), and 3.84 ppm (6H).

Reaction of an orange CD_3CN solution of $K^+(18\text{-crown-6})[CpCr(CO)_2(Ime)]^{-1/2}THF$ with the acid $[H\text{-DBU}]^+BF_4^-$ ($pK_a^{MeCN} = 24.3$, DBU = 1,8-diazabicyclo[5.4.0]undec-7-ene)²⁴ or with $NH_4^+PF_6^-$ ($pK_a^{MeCN} = 16.5$)²⁵ resulted in a light yellow solution, giving new 1H NMR resonances at 7.09 (2H), 4.63 (5H), 3.78 (6H), and -5.33 ppm (1H), which we assigned to the hydride $CpCr(CO)_2(Ime)H$ (Scheme 1). Although the hydride is drawn in Scheme 1 with cis geometry, we cannot draw any conclusions on the geometry based on the available data.²⁶ Integration of these resonances against the "internal standard" 18-crown-6 (24H) showed that the hydride is

produced in about 95% yield. Although the hydride was generated cleanly, it is not thermodynamically stable; IR signals due to $CpCr(CO)_2(Ime)^*$ always became noticeable after 10–60 min, and grew in intensity at the expense of the signals due to $CpCr(CO)_2(Ime)H$. A 45 mM solution of $CpCr(CO)_2(Ime)H$ in CD_3CN was found by 1H NMR spectroscopy to be 75% decomposed after 1 day at room temperature. $CpCr(CO)_2(Ime)^*$ was identified as the major organometallic product, and a weak singlet at 4.57 ppm was observed for H_2 . The same observations were made when a solution of $CpCr(CO)_2(Ime)H$ was maintained in the dark. We were unable to isolate samples of $CpCr(CO)_2(Ime)H$ because of its instability, which seems to increase at higher concentrations. For example, removal of volatiles from a freshly generated Et_2O/THF solution of $CpCr(CO)_2(Ime)H$ gave a residue which, by IR spectroscopy, consisted of less than 20% of the hydride, the remainder being the 17-electron radical. Thus, attempts to isolate pure $CpCr(CO)_2(Ime)H$ were fruitless.

Scheme 2



The equilibrium constant for the protonation reaction of $\text{K}^+(18\text{-crown-6})[\text{CpCr}(\text{CO})_2(\text{Ime})]^{-1/2}\text{THF}$ (10 mM $[\text{Cr}]$) was determined in CD_3CN with the acid $[\text{H}^t\text{BuP}_1(\text{pyrr})]^+\text{BF}_4^-$ ($\text{p}K_{\text{a}}^{\text{MeCN}} = 28.4$, ${}^t\text{BuP}_1(\text{pyrr}) = (\text{tert-butylimino})\text{tris}(1\text{-pyrrolidinyl})\text{phosphorane}$).^{24,27} ${}^1\text{H}$ NMR and IR spectroscopy suggested that the protonation equilibrium is established rapidly. Two ${}^1\text{H}$ NMR equilibrium measurements with different acid concentrations gave the same protonation equilibrium constant ($K = 0.06$); thus, the $\text{p}K_{\text{a}}^{\text{MeCN}}$ of the hydride was determined to be 27.2. The unavailability of clean samples of $\text{CpCr}(\text{CO})_2(\text{Ime})\text{H}$ prevented us from approaching the equilibrium from the opposite direction. Therefore, we conservatively assign a relatively large uncertainty of ± 0.4 in the quoted $\text{p}K_{\text{a}}^{\text{MeCN}}$ of $\text{CpCr}(\text{CO})_2(\text{Ime})\text{H}$.

$\text{CpCr}(\text{CO})_2(\text{PCy}_3)^{\bullet}$, $[\text{CpCr}(\text{CO})_2(\text{PCy}_3)]^{-}$, and $\text{CpCr}(\text{CO})_2(\text{PCy}_3)\text{H}$. We also synthesized (Scheme 2) an analogous series of complexes containing the tricyclohexylphosphine ligand, one of the more electron-donating and bulky²⁸ phosphines. The reaction of $[\text{CpCr}(\text{CO})_3]_2$ with PCy_3 in $\text{MeCN}/\text{Et}_2\text{O}$ at $20\text{ }^{\circ}\text{C}$ proceeded slowly, but cleanly provided $\text{CpCr}(\text{CO})_2(\text{PCy}_3)^{\bullet}$ in about 65% yield as a yellow/orange crystalline precipitate over the course of several days. The room temperature EPR spectrum in toluene displays a broad doublet at $g_{\text{iso}} = 2.035$ ($A_{\text{iso}}({}^{31}\text{P}) = 94\text{ MHz}$), which sharpens upon cooling. Like the Ime analogue, $\text{CpCr}(\text{CO})_2(\text{PCy}_3)^{\bullet}$ exhibits Curie paramagnetic behavior in solution. (Relevant spectra and figures can be found in the Supporting Information.)

Electrochemically, $\text{CpCr}(\text{CO})_2(\text{PCy}_3)^{\bullet}$ is reversibly reduced to $\text{CpCr}(\text{CO})_2(\text{PCy}_3)^{-}$ at $E_{1/2} = -1.58(1)\text{ V}$ vs $\text{Cp}_2\text{Fe}^{+/0}$ in MeCN . Treatment of the radical with KC_8 and 18-crown-6 provided $\text{K}^+(18\text{-crown-6})[\text{CpCr}(\text{CO})_2(\text{PCy}_3)]^{-}$ in 90% yield as a yellow powder. Protonation with $\text{NH}_4^+\text{PF}_6^-$ in MeCN cleanly provided $\text{CpCr}(\text{CO})_2(\text{PCy}_3)\text{H}$. Because of its low solubility in MeCN , it precipitates from the reaction mixture, and was isolated as light yellow crystals in 80% yield. In the ${}^1\text{H}$ NMR spectrum in CD_3CN , the signal due to the hydride is a doublet (${}^2J_{\text{HP}} = 80\text{ Hz}$) at -6.22 ppm ; the large H-P coupling constant suggests that the *cis* isomer is the predominant isomer.²⁹ The $\text{p}K_{\text{a}}^{\text{MeCN}}$ of $\text{CpCr}(\text{CO})_2(\text{PCy}_3)\text{H}$ was determined to be 26.1(3), using the phosphazene base (*tert*-butylimino)tris(dimethylamino)phosphorane (${}^t\text{BuP}_1(\text{dma})$,

$\text{p}K_{\text{a}}^{\text{MeCN}}$ of conjugate acid = 26.98²⁴); the equilibrium was approached from both directions.

Orange crystals of $\text{CpCr}(\text{CO})_2(\text{PCy}_3)^{\bullet}$ and light yellow crystals of *cis*- $\text{CpCr}(\text{CO})_2(\text{PCy}_3)\text{H}$, suitable for X-ray diffraction, were grown from supersaturated MeCN solutions. The molecular structures are shown in Figure 9, and selected

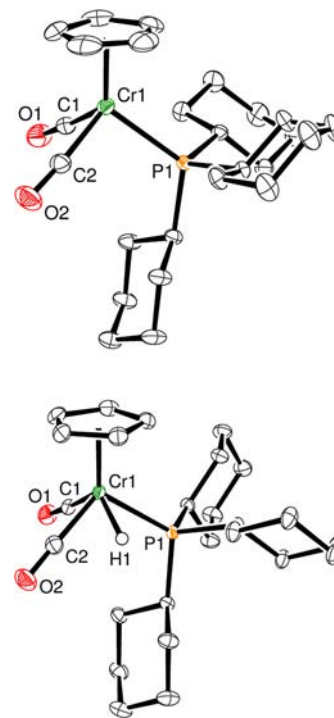


Figure 9. Molecular structures of $\text{CpCr}(\text{CO})_2(\text{PCy}_3)^{\bullet}$ (top) and $\text{CpCr}(\text{CO})_2(\text{PCy}_3)\text{H}$ (50% probability ellipsoids; C-bonded hydrogens omitted).

metrical parameters are provided in Table 3. In *cis*- $\text{CpCr}(\text{CO})_2(\text{PCy}_3)\text{H}$, the hydride was located and refined, although it should be kept in mind that its position is not obtained with accuracy in an X-ray diffraction experiment.³⁰ Nevertheless, the presence of an additional ligand (as compared to the radical) is also clearly revealed by the C1–Cr1–P1 and C2–Cr1–P1

Table 3. Bond Lengths (Å) and Angles (deg) for CpCr(CO)₂(PCy₃)[•] and CpCr(CO)₂(PCy₃)H

	CpCr(CO) ₂ (PCy ₃) [•]	CpCr(CO) ₂ (PCy ₃)H
Cr1–Cp _{centroid}	1.854(1)	1.852(1)
Cr1–P1	2.3760(6)	2.3315(4)
Cr1–C1, Cr1–C2	1.827(2), 1.838(2)	1.823(2), 1.819(2)
C1–O1, C2–O2	1.158(3), 1.159(3)	1.163(2), 1.165(2)
Cr1–H1	NA	1.53(2) ³⁰
C1–Cr1–C2	79.64(9)	82.85(7)
C1–Cr1–P1	94.40(7)	84.62(5)
C2–Cr1–P1	97.67(7)	107.77(5)

angles, which become significantly different in going from the radical to the hydride.

Thermochemistry: Cr–H BDFE and Thermodynamics of H₂ Loss. Equations 3 and 4 demonstrate how the M–H homolytic bond dissociation free energy (BDFE) and the BDE (enthalpy) can be derived from the thermodynamic acidities of hydrides and the formal potentials of M^{•/–} electrochemical couples in acetonitrile solvent.^{31,32} Because the M^{•/–} wave is fully reversible (Figure 5), we assume that the formal potential (*E*^o) is the same as the half-wave potential (*E*_{1/2}). The results for this thermochemical analysis for CpCr(CO)₂(L)H are detailed in Scheme 3. Additionally, using the homolytic bond dissociation free energy of H₂ (103.6 kcal mol^{–1}),³¹ the thermodynamic stability of the hydrides with respect to loss of dihydrogen, in the overall reaction 2 Cr–H → 2 Cr[•] + H₂, was evaluated.³³

$$\begin{aligned} \text{BDFE} &= \Delta G_{\text{H}}(\text{MH}) \\ &= 1.37 \text{ p}K_{\text{a}}(\text{MH}) + 23.06 E^{\circ}(\text{M}^{\bullet/ -}) + 53.6 \end{aligned} \quad (3)$$

$$\begin{aligned} \text{BDE} &= \Delta H_{\text{H}}(\text{MH}) \\ &= 1.37 \text{ p}K_{\text{a}}(\text{MH}) + 23.06 E^{\circ}(\text{M}^{\bullet/ -}) + 59.5 \end{aligned} \quad (4)$$

DISCUSSION

17-Electron Chromium Complexes. Whereas CpCr(CO)₂(PCy₃)[•] is a bulky addition to a family of well-characterized^{34–36} complexes CpCr(CO)₂(PR₃)[•], carbene analogues CpCr(CO)₂(NHC)[•] were heretofore not known. This is perhaps surprising, considering that isoelectronic (yet cationic) complexes Cr(CO)₄(NHC)₂^{•+} were reported in 1983 by Hofmann, Öfele and co-workers, and considering that Cr(CO)₅(Ime), the first transition metal NHC complex, was

reported in 1968.³⁷ Fortier, Macartney, Baird and co-workers have established that reactions of [CpCr(CO)₃]₂ with PR₃ involve the monomer CpCr(CO)₃[•] (which is in equilibrium³⁸ with the dimer), and that the substitution proceeds by an associative mechanism.³⁴ We assume that this mechanism is also operative in the synthesis of the radicals reported here. On the basis of the timescales during which the reactions take place (seconds for IMe, days for PCy₃), we conclude that IMe is the superior nucleophile. IMe is also the better electron donor, as judged by $\tilde{\nu}_{\text{CO}}$ values that are $\approx 10 \text{ cm}^{-1}$ lower for CpCr(CO)₂(Ime)[•] than for CpCr(CO)₂(PCy₃)[•] (Table 1, entries 1 and 2).

The monomeric nature of both radicals was expected, and unequivocally established by the crystal structure analyses. For CpCr(CO)₂(Ime)[•], the four statistically identical Cr–C_(carbene) bond lengths of 2.05 Å are at the short end of the range of 2.04–2.25 Å found for other crystallographically characterized³⁹ N-heterocyclic carbene complexes of chromium. However, they are still > 0.2 Å longer than the Cr–C_(CO) bonds (1.80–1.82 Å), and can be regarded as Cr–C single bonds, as would be expected for the singlet carbenes. Compared to the carbene complex, the phosphorus atom in CpCr(CO)₂(PCy₃)[•] is placed at a significantly larger distance from chromium (*d* = 2.3760(6) Å): this Cr–P distance is also 0.031(1) Å longer than in CpCr(CO)₂(PPh₃)[•].³⁵ In both structures, key features are the small (76–80°) C_{CO}–Cr–C_{CO} angles in comparison to much larger (94–101°) C_(carbene)–Cr–C_(CO) or P–Cr–C_(CO) angles. Such an irregular placement of the three legs of the piano-stool has precedent in related phosphine-ligated radicals,^{35,36,40} and shows that the effectively C_s-symmetric radicals have ²A'' electronic ground states. The orientation of the IMe and PCy₃ ligands is such that steric repulsion with the CpCr(CO)₂ fragment is minimized, which is accomplished in different ways because of the differing rotational symmetries of these ligands (2- and 3-fold, respectively). Thus, in CpCr(CO)₂(Ime)[•] the approximate mirror plane bisects the carbene ligand, an orientation that we previously found¹⁰ by DFT calculations for the heavier congener CpW(CO)₂(Ime)[•]. In CpCr(CO)₂(PCy₃)[•], the pseudo-3-fold CpCr(CO)₂ fragment is staggered with respect to the PCy₃ ligand.

The EPR spectra of the radicals are in most aspects similar to the spectra for CpCr(CO)₂(PPh₃)[•] and related low-spin, d⁵ piano-stool complexes;^{36,41} frozen solution spectra are rhombic, and one of the principal *g* values is smaller than the free-electron value (2.0023). The radicals are largely Cr-centered as expected, but for CpCr(CO)₂(Ime)[•] it is further corroborated

Scheme 3. Thermochemical Data for CpCr(CO)₂(L)H^a

		ΔG (kcal mol ^{–1})	
		L = IMe	L = PCy ₃
CrH	→ Cr [•] + H [•]	$\Delta G_{\text{H}}(\text{CrH})$	= 37.3(5) 35.8(4)
Cr [•]	→ Cr ^{•+} + e [–]	$-\Delta G(\text{Cr}^{\bullet/ -})$	= –43.6(2) –36.4(2)
H [•] + e [–]	→ H [•]	$\Delta G(\text{H}^{\bullet/ -})$ ^{31,32}	= 53.6 53.6
CrH	→ Cr[•] + H[•]	$\Delta G_{\text{H}}(\text{CrH})$	(BDFE) = 47.3(6) 52.9(4)
		$\Delta H_{\text{H}}(\text{CrH})$	(BDE) = 53.2(6) 58.8(4)
2 CrH	→ 2 Cr [•] + 2 H [•]	$2\Delta G_{\text{H}}(\text{CrH})$	= 94.6(8) 105.8(6)
2 H [•]	→ H ₂	$\Delta G_{\text{H}_2}(2\text{H}^{\bullet})$ ³¹	= –103.6 –103.6
2 CrH	→ 2 Cr[•] + H₂	$\Delta G_{\text{H}_2+2\text{Cr}}(2\text{CrH})$	= –9.0(8) +2.2(6)

^aMeCN solvent, *T* = 293 K.

by the observation of hyperfine coupling to ^{53}Cr . The g -anisotropy ($g_{\text{max}} - g_{\text{min}}$) is significantly smaller for the carbene complex (0.073) than for the phosphine-ligated $\text{CpCr}(\text{CO})_2(\text{PCy}_3)^{\bullet}$ (0.096) and $\text{CpCr}(\text{CO})_2(\text{PPh}_3)^{\bullet}$ (0.113).⁵⁶ It is noteworthy that room temperature EPR signals for $\text{CpCr}(\text{CO})_2(\text{IME})^{\bullet}$ and $\text{CpCr}(\text{CO})_2(\text{PCy}_3)^{\bullet}$ are so easily observed, considering that efficient electron spin–lattice relaxation can cause extreme broadening (often to the point of unobservability) of room temperature signals in related Cr piano-stool radicals. We think that the NIR spectra provide at least a qualitative explanation. Atwood and Geiger reported¹⁷ that 17-electron piano-stool radicals have a weak ($\epsilon \approx 100 \text{ M}^{-1} \text{ cm}^{-1}$) electronic transition in the near- to mid-IR region, which is probably best thought of as an interconversion between $^2\text{A}''$ and $^2\text{A}'$ electronic states. Whereas λ_{max} for this transition is at 2500 nm for $(\text{C}_5\text{Ph}_5)\text{Cr}(\text{CO})_3^{\bullet}$, tailing into the mid-IR,¹⁷ we find it at 1455 nm for $\text{CpCr}(\text{CO})_2(\text{IME})^{\bullet}$ and at 1660 nm for $\text{CpCr}(\text{CO})_2(\text{PCy}_3)^{\bullet}$ (Figure 2), that is, at considerably higher energy. Therefore, it is possible that the interconversion between $^2\text{A}''$ and $^2\text{A}'$ electronic states, and hence the electron spin–lattice relaxation efficiency, is drastically reduced in the radicals reported here.

The Curie paramagnetic behavior that we find by variable temperature ^1H NMR spectroscopy for $\text{CpCr}(\text{CO})_2(\text{IME})^{\bullet}$ and $\text{CpCr}(\text{CO})_2(\text{PCy}_3)^{\bullet}$ was previously also found for $\text{CpCr}(\text{CO})_3^{\bullet}$ and $(\text{C}_5\text{Me}_5)\text{Cr}(\text{CO})_3^{\bullet}$ in an elegant study by Wayland and co-workers.⁴² The latter two radicals are involved in temperature-dependent equilibria with the diamagnetic dimers, which complicates the analysis, although the authors successfully accounted for the dimerization. The strictly monomeric nature of our radicals makes the analyses straightforward; furthermore, they provide information on multiple types of protons instead of one. The hyperfine shifts in the ^1H NMR spectra appear to be predominantly caused by Fermi contact coupling of the nuclei with the electron, dipolar (pseudocontact) interactions being less important. For example, were the latter dominant, we would have expected for $\text{CpCr}(\text{CO})_2(\text{IME})^{\bullet}$ that the carbene CH_3 signal would be shifted to a greater extent than the carbene CH signal, because of the different $\text{Cr}\cdots\text{H}$ separations ($d(\text{Cr}\cdots\text{H}_3\text{C}) = 3.1\text{--}4.5 \text{ \AA}$; $d(\text{Cr}\cdots\text{HC}) = 5.1 \text{ \AA}$); however, the opposite is observed (Figure 3).

Electron-Rich Anions $\text{CpCr}(\text{CO})_2(\text{IME})^-$ and $\text{CpCr}(\text{CO})_2(\text{PCy}_3)^-$. The difference in electron-richness of the IME and PCy_3 complexes, already substantial in the neutral radicals, seems to be even larger in the anions. Comparison between entries 4 and 5 of Table 1 shows that $\tilde{\nu}_{\text{CO}}$ values differ by about 25 cm^{-1} in the anions, where the difference is about 10 cm^{-1} in the radicals. Also, while $\text{CpCr}(\text{CO})_2(\text{PCy}_3)^-$ is quite reducing ($E^\circ = -1.58(1) \text{ V}$ vs $\text{Cp}_2\text{Fe}^{+/0}$, 70 mV more negative than the PEt_3 derivative⁴³), it is easily surpassed by $\text{CpCr}(\text{CO})_2(\text{IME})^-$ ($-1.89(1) \text{ V}$ vs $\text{Cp}_2\text{Fe}^{+/0}$). The latter redox potential is also about 0.35 V more negative than that of the tungsten derivative $\text{CpW}(\text{CO})_2(\text{IME})^{\bullet/-}$ ($-1.54(2) \text{ V}$ vs $\text{Cp}_2\text{Fe}^{+/0}$);¹² differences of about 0.3 V between Cr and Mo/W congeners are documented for the parent anions $\text{CpM}(\text{CO})_3^{\bullet/-}$.¹³

The highly reducing nature of the anions is also the (indirect) cause of their broadened NMR spectra. Dissolution of the salts in MeCN adventitiously generates small amounts (ca. 1–2%, observed in IR spectrum) of the radical, with which the anion is in rapid electron-transfer exchange. The hypothesis is confirmed by the observed sharpening of the signals when KC_8 is added, reducing any radical that is present back to the

anion; similar observations were made for $\text{CpW}(\text{CO})_2(\text{IMes})^-$.¹⁰

As expected, the crystal structures of both $\text{K}^+[\text{CpCr}(\text{CO})_2(\text{IME})]^-$ salts, with and without the crown ether, show contact ion pairing through $\text{K}\cdots\text{O}_{(\text{CO})}$ interactions. Because both structures contain more than one (two and four, respectively) crystallographically independent ion pairs in the asymmetric unit, the relative structural flexibility of these interactions became apparent. In $\text{K}^+(18\text{-crown-6})[\text{CpCr}(\text{CO})_2(\text{IME})]^- \cdot 1/2\text{THF}$, for example, the potassium in one ion pair is pinched by two Cr-bound carbonyls, while in the other it is ligated by only one Cr-bound carbonyl. Precedent for these respective situations is found in the structures of $\text{K}^+(18\text{-crown-6})[\text{CpW}(\text{CO})_2(\text{IMes})]^-$ ¹⁰ and $\text{K}^+(18\text{-crown-6})-[(\text{C}_5\text{H}_4\text{CH}_2\text{CH}_2\text{PPh}_2)\text{M}(\text{CO})_3]^-$ ($\text{M} = \text{Cr}, \text{Mo}, \text{W}$).⁴⁴ The potassium cation accommodates this reduction in the number of bonded donors by binding more strongly to the remaining donors (see Table 2). The pinching vs nonpinching interactions are probably the cause of the significantly different $\text{C}_{\text{CO}}\text{--Cr--C}_{\text{CO}}$ angles.

The structure of crown-free $\text{K}^+[\text{CpCr}(\text{CO})_2(\text{IME})]^- \cdot 3/4\text{THF}$ shows that the anion-based ligands (largely the carbonyls) alone almost succeed in filling the coordination spheres of the potassium cations—just one in twenty $\text{K}\cdots\text{O}$ interactions is due to a THF ligand, and two-thirds of the THF molecules present are lattice solvents that do not interact with potassium at all. In fact, there are crystal structures of K^+ salts of related $\text{M}(0)$ anions (for example, $\text{K}^+[\text{CpFe}(\text{CO})_2]^-$ ⁴⁵ and $\text{K}^+[\text{CpMo}(\text{CO})_3]^-$ ⁴⁶) that are entirely free of additional Lewis bases. On average, the $\text{K}\cdots\text{O}_{(\text{CO})}$ interactions are stronger in the crown-free ($d(\text{K}\cdots\text{O}_{(\text{CO})})_{\text{av}} = 2.77 \text{ \AA}$) than in the crown-containing ($d(\text{K}\cdots\text{O}_{(\text{CO})})_{\text{av}} = 2.94 \text{ \AA}$) material. This is probably related to the differing number of O ligands surrounding K^+ in both structures: seven and eight in the latter, and a maximum of six in the former. Further, the Cr–C and C–O bond lengths (Table 2) may suggest that there is more metal-to-carbonyl backbonding in the crown-free ($d(\text{Cr--C})_{\text{av}} = 1.773 \text{ \AA}$, $d(\text{C--O})_{\text{av}} = 1.207 \text{ \AA}$) than in the crown-containing ($d(\text{Cr--C})_{\text{av}} = 1.778 \text{ \AA}$, $d(\text{C--O})_{\text{av}} = 1.200 \text{ \AA}$) structure, in line with the expectation⁴⁷ that stronger $\text{K}\cdots\text{O}_{(\text{CO})}$ interactions should encourage backbonding. However, this point has to be made with caution: although the values are averages of four or eight individual bond lengths, it is hard to establish how significant the differences are.

The IR data give qualitative information about the nature of the $\text{K}^+[\text{CpCr}(\text{CO})_2(\text{IME})]^-$ salts in solution. We make the assumption that $\text{K}^+(18\text{-crown-6})[\text{CpCr}(\text{CO})_2(\text{IME})]^- \cdot 1/2\text{THF}$ exists largely as solvent-separated ion pairs in MeCN, a polar and high-dielectric ($\epsilon_r = 37.5$) solvent. In THF ($\epsilon_r = 7.5$), the low-energy band appears at lower energy than in MeCN, a behavior that contrasts that of the neutral species $\text{CpCr}(\text{CO})_2(\text{IME})^{\bullet}$ and $\text{CpCr}(\text{CO})_2(\text{IME})\text{H}$, in which the bands shift to higher energy upon going from MeCN to THF (Table 1). As Darensbourg has shown that the interaction of a carbonyl oxygen with an alkali metal cation will decrease its $\tilde{\nu}_{\text{CO}}$,⁴⁷ we interpret our observation as a sign that $\text{K}^+(18\text{-crown-6})[\text{CpCr}(\text{CO})_2(\text{IME})]^- \cdot 1/2\text{THF}$ remains somewhat ion-paired in solution. Crown-free $\text{K}^+[\text{CpCr}(\text{CO})_2(\text{IME})]^-$ may be undergoing some ion-pairing even in MeCN, as its $\tilde{\nu}_{\text{CO}}$ bands are somewhat broader (yet hardly shifted) than in the crown-containing derivative. In THF, both bands are now shifted to lower energy, which suggests that the absence of the crown ether causes both carbonyls to interact with K^+ in THF. In light

of the polymeric nature of crown-free $K^+[CpCr(CO)_2(Ime)]^-$ in the solid state, as determined crystallographically, it is possible that ion pair aggregation occurs in solution.

Hydrides with Weak Cr–H Bonds. The Cr–H bond properties of the hydrides described herein can be compared with those of the parent $CpCr(CO)_3H$, since its Cr–H BDE has been reliably determined to be 61–62 kcal mol⁻¹ by calorimetry.¹⁴ This bond strength is also obtained by thermochemical analysis: its pK_a^{MeCN} (13.3)⁴⁸ and E° for the couple $CpCr(CO)_3^{*/-}$ (–0.688 V vs $Cp_2Fe^{*/0}$)¹³ provide, using Equations 3 and 4, a BDFE value of 56.0 kcal mol⁻¹ and a BDE value of 61.9 kcal mol⁻¹. Hoff and co-workers found that the Cr–H BDEs of several phosphine/phosphite derivatives $CpCr(CO)_2(PR_3)H$ (R = Ph, 59.8; Et, 59.9; OMe, 62.7 kcal mol⁻¹) are not very different from that of $CpCr(CO)_3H$.¹⁴ Our determined Cr–H BDE for $CpCr(CO)_2(Ime)H$ (53.2(6) kcal mol⁻¹) is not only significantly lower than that of the aforementioned hydrides, it is even lower than the 55–58 kcal mol⁻¹ that Norton and co-workers⁹ found for a series of vanadium hydrides $HV(CO)_4(Ph_2P(CH_2)_nPPh_2)$ ($n = 1-4$). Thus, the Cr–H bond in $CpCr(CO)_2(Ime)H$ appears to be the weakest M–H bond observed among organometallic hydrides. On the other hand, the Cr–H bond in $CpCr(CO)_2(PCy_3)H$ is only about 3 kcal mol⁻¹ weaker than the Cr–H bond in $CpCr(CO)_3H$, and about 1 kcal mol⁻¹ weaker than that in $CpCr(CO)_2(PPh_3)H$.

Inspection of Scheme 3 reveals that the 5.6(7) kcal mol⁻¹ higher BDFE for $CpCr(CO)_2(PCy_3)H$ as compared to $CpCr(CO)_2(Ime)H$ is mainly caused by the large difference in formal potentials of the $[Cr]^{*/-}$ couples. The pK_a^{MeCN} of the hydrides (as expected, both higher than the 21.8 determined for $CpCr(CO)_2(PPh_3)H$)⁴⁹ differ by only 1.1(5) units, and are remarkably similar considering our recent observation that substitution of PMe_3 for either Ime or $IMes$ (1,3-dimesitylimidazol-2-ylidene) increases the pK_a of related tungsten hydrides by about 5 units.^{11,12} Admittedly, this is not a direct comparison, and we should assume that substitution of PMe_3 for PCy_3 itself will somewhat lower the thermodynamic acidity of metal hydrides, taking into account that PCy_3 is a better donor²⁸ than PMe_3 .

The experimentally observed (in)stabilities of our hydrides are in agreement with the thermochemical analysis (Scheme 3). Thus, $CpCr(CO)_2(Ime)H$ should not be stable with respect to formation of the 17-electron radical and H_2 . Indeed, we can only characterize $CpCr(CO)_2(Ime)H$ in solution. We find that it slowly decomposes to form the radical, and attempts to isolate the hydride have been unsuccessful. Since the same result is obtained when the sample is shielded from light, we conclude that the decomposition is a thermal process. On the other hand, $CpCr(CO)_2(PCy_3)H$ was relatively easily characterized and obtained in analytically pure form. The non-observation of $CpCr(CO)_2(Ime)H$ in the reaction of $CpCr(CO)_2(Ime)^*$ with excess H_2 (1000 psi) in principle also agrees with the thermochemical analysis. However, we do not know the kinetics of the hydrogenation reaction, and that experiment on its own would have been inconclusive with regard to the thermochemistry.

Why is the Cr–H bond in $CpCr(CO)_2(Ime)H$ so weak? Sirsch, McGrady and co-workers have demonstrated that even the hydride $CpCr(CO)_3H$ has a sterically crowded basal ligand set,⁵⁰ while Skagestad and Tilset have noted that extremely bulky ligands may increase thermodynamic acidities of hydrides.⁵¹ Therefore, we think that extreme steric crowding

in $CpCr(CO)_2(Ime)H$ is an important factor in causing its very low Cr–H BDFE and its comparatively high acidity. Although PCy_3 is a bulky ligand, its 3-fold rotational symmetry allows it to gear quite effectively with the $CpCr(CO)_2H$ fragment (Figure 9); such gearing is less optimal for the Ime ligand with its 2-fold rotational symmetry. For example, we characterized the stable *cis*- $CpW(CO)_2(Ime)H$ by X-ray diffraction, and found that one N-methyl is rather close to the hydride ($d(WH\cdots CH_3) = 2.43(4)$ Å).¹² An increased crowding can be expected for the chromium analogue, because $M-C_{(carbene)}$, $M-C_{(Cp)}$, and $M-C_{(CO)}$ distances are about 0.15 Å shorter for Cr than for W. Although we have not been able to address the issue of *cis/trans* isomerism in $CpCr(CO)_2(Ime)H$, either isomer can be expected to have close interactions of an N-methyl group with another basal ligand, as illustrated in Figure 10.⁵²

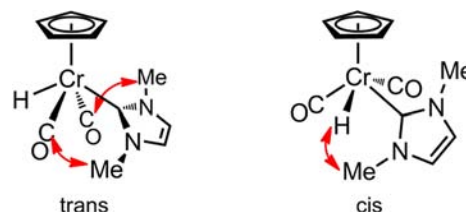


Figure 10. Steric interactions of N-CH₃ groups with other basal ligands in $CpCr(CO)_2(Ime)H$.

CONCLUSIONS

A full synthetic and spectroscopic and characterization of chromium piano-stool chromium hydrides $CpCr(CO)_2(L)H$ (L = PCy_3 , Ime), as well as derived anions and 17-electron radicals, has been reported. Thermochemical analyses correctly predict the stability of these hydrides with respect to H atom loss in the form of dihydrogen. $CpCr(CO)_2(Ime)H$ is unstable in this regard, because its Cr–H BDFE is only 47.3(6) kcal mol⁻¹, nearly 6 kcal mol⁻¹ lower than that of $CpCr(CO)_2(PCy_3)H$. The comparison suggests the intriguing possibility that while the free ligand Ime is much smaller and more nucleophilic than PCy_3 , the carbene exerts a greater steric pressure on the other ligands than the phosphine does, once incorporated in the coordination sphere.

EXPERIMENTAL SECTION

General Procedures. All manipulations were carried out under N_2 using standard vacuum line, Schlenk, and inert-atmosphere glovebox techniques. Acetonitrile, diethyl ether, hexanes, fluorobenzene, tetrahydrofuran, and toluene were purified by passage through neutral alumina, using an Innovative Technology, Inc., Pure Solv solvent purification system. Hexafluorobenzene (>99%, Aldrich) was stirred over P_2O_5 and vacuum transferred. Deuterated solvents (Cambridge Isotope Laboratories, 99.5% D or greater) were dried as follows: toluene- d_8 was vacuum transferred from sodium-potassium alloy; CD_3CN was stirred over P_2O_5 and then vacuum distilled through a glass wool plug. Tetrabutylammonium hexafluorophosphate (anhydrous, >99%, Fluka), ammonium hexafluorophosphate (>98%, Fluka), DBU (>99%, Fluka), Schwesinger bases $tBuP_1(pyrr)$ and $tBuP_1(dma)$ (Fluka), ferrocene (Aldrich), and cobaltocene (Strem) were used as received. Potassium hydride was obtained as a 30 wt % suspension in mineral oil; in the glovebox, the mineral oil was washed away with hexanes, and the KH was dried under vacuum. KC_8 was obtained by heating potassium and graphite (1:8 mol ratio) to 200 °C. Acids $[H-DBU]^+BF_4^-$, $[H^tBuP_1(dma)]^+OTf^-$, and $[H^tBuP_1(pyrr)]^+BF_4^-$ were prepared by protonation of the conjugate bases with ethereal HBF_4 (or

HOTf) in Et₂O. The resulting white precipitates were purified by precipitation from THF or MeCN by addition of Et₂O, and washed with Et₂O. Tricyclohexylphosphine (Strem) was sublimed at 90 °C at <1 mTorr onto a water-cooled finger. [CpCr(CO)₃]₂,⁵³ and 1,3-dimethylimidazolium iodide⁵⁴ were prepared as described in the literature. Elemental analyses were performed by Atlantic Microlab (Norcross, GA). Low %C analyses were obtained for the highly air-sensitive and easily oxidizable anionic Cr⁰ complexes, an issue we also encountered for related tungsten complexes.¹² Uncertainties in the measured pK_a and E° values, as well as in the derived thermochemical energy data, are provided at the 2σ confidence interval.

Instrumentation. Electrochemical measurements were performed using a CH Instruments potentiostat equipped with a standard three-electrode cell consisting of a 4 mL disposable glass vial fitted with a polyethylene cap having openings sized to closely accept each electrode. For each experiment, the cell was assembled and used within the glovebox, with electrodes connected to the potentiostat via RF-shielded cables fed through the glovebox wall. The working electrode (1 mm PEEK-encased glassy carbon, Cypress Systems EE040) was polished using alumina (BAS CF-1050, dried at 150 °C under vacuum) suspended in acetonitrile, and then rinsed with neat acetonitrile. A glassy carbon rod (Structure Probe, Inc.) was used as the counterelectrode, and a silver wire suspended in a solution of 0.1 M ^tBu₄N⁺PF₆⁻ in acetonitrile and separated from the analyte solution by a porous Teflon tip (CH Instruments 112) was used as the pseudoreference electrode. Potentials are reported vs the Cp₂Fe^{+•/0} couple, and were determined versus cobaltocene (E° = -1.33 V vs Cp₂Fe^{+•/0}). NMR experiments were carried out using Varian 300 or 500 MHz spectrometers. ¹H and ¹³C NMR spectra were referenced relative to NMR solvent (protic residual for ¹H) peaks. ³¹P NMR spectra were referenced with respect to a referenced ¹H NMR spectrum with the use of Varian's *mref* command. EPR spectra were recorded at or below 1 mM (making sure that further dilution did not result in a change in signal shape) in liquid or frozen toluene solutions, using a Bruker Elexsys X-band EPR spectrometer equipped with a helium-cooled cryostat; g values were derived from the field/frequency ratios, and simulations were performed with EasySpin.⁵⁵ Solution IR spectra (data are provided in Table 1) were recorded using a Nicolet iS10 FTIR spectrometer with demountable sealed liquid CaF₂ cells (International Crystal Laboratories). Solid-state IR spectra were measured as nujol mulls between CaF₂ plates. Vis-NIR spectra were recorded on an Agilent Cary 5000 UV-vis-NIR spectrometer, using quartz cuvettes with 10 mm path length.

Synthesis of CpCr(CO)₂(Ime)[•]. 1,3-Dimethylimidazolium iodide (0.426 g, 1.90 mmol) and KH (0.206 g, 5.1 mmol) were placed in a 20 mL vial, and the suspension was stirred in THF (3 mL). Slow evolution of a gas (presumably H₂) was observed. After 4 h, effervescence had stopped, and Et₂O (10 mL) was added to ensure nearly complete precipitation of the KI. The solution of the generated 1,3-dimethylimidazol-2-ylidene was filtered and added, in portions of about 0.5 mL, to a dark green suspension of [CpCr(CO)₃]₂ (0.261 g, 0.649 mmol, corresponding to 1.30 mmol monomeric CpCr(CO)₃[•]) in Et₂O (2 mL). Addition of portions of the Ime solution each time resulted in effervescence and a temporary color change from green to orange/yellow; the green color then reappeared because of dissolution of remaining starting material. When the green color did not reappear (a sign that the starting material was consumed), the addition of the Ime solution was stopped. The resulting solution, containing an unidentified fluffy precipitate, was filtered into 3 mL of hexane, affording an orange, cloudy solution. Under reduced pressure, the volume was reduced to about 5 mL. (The crude solution of CpCr(CO)₂(Ime)[•] should not be evaporated to dryness; the oily residue suddenly turns black and becomes intractable. The extent and cause of this apparent decomposition was not investigated further, but it is possible that excess free Ime is involved. Once CpCr(CO)₂(Ime)[•] has solidified, it is thermally stable and readily handled.) Hexane (5 mL) was added, and the volume was again reduced to about 5 mL. This procedure of hexane addition and concentration was repeated twice to remove most of the Et₂O and THF. Most of the product had precipitated as an orange, viscous liquid. Vigorous stirring and scraping

eventually resulted in solidification, to give an orange-brown powder suspended in a yellow solution. After cooling to -35 °C overnight, the powder was filtered, washed with hexane (2 × 5 mL), and dried under vacuum. Sublimation at 100–110 °C at <1 mTorr onto a water-cooled finger gave the analytically pure product as an orange/brown powder. Yield: 0.277 g (1.03 mmol, 79%). ¹H NMR (CD₃CN, 500 MHz, 295 K): δ ≈ 31.1 (br, fwhm ≈ 4500 Hz, 2H, =CH), 13.1 (br, fwhm = 690 Hz, 5H, Cp), 4.9 (br, fwhm = 210 Hz, 6H, N-CH₃). ¹H NMR (toluene-d₈, 500 MHz, 295 K): δ ≈ 30.7 (br, fwhm ≈ 4500 Hz, 2H, =CH), 12.9 (br, fwhm = 690 Hz, 5H, Cp), 3.1 (br, fwhm = 240 Hz, 6H, N-CH₃). Anal. Calcd. for C₁₂H₁₃N₂O₂Cr: C, 53.53; H, 4.87; N, 10.40. Found: C, 53.33; H, 4.92; N, 10.53. Single crystals of CpCr(CO)₂(Ime)[•] were grown by diffusion of hexane into a fluorobenzene solution of it at room temperature. An oily precipitate was initially obtained, from which orange rods grew over the course of several days.

Synthesis of CpCr(CO)₂(PCy₃)[•]. A solution of PCy₃ (0.170 g, 0.606 mmol) in Et₂O (1 mL) was added to a dark green suspension of [CpCr(CO)₃]₂ (0.110 g, 0.273 mmol, corresponding to 0.547 mmol monomeric CpCr(CO)₃[•]) in MeCN (3 mL). The suspension was stirred at room temperature for two days to afford the product as a yellow/orange precipitate, which was washed with MeCN (3 × 3 mL) and dried under vacuum to give a yellow/orange powder. Yield: 0.160 g (0.353 mmol, 65%). ¹H NMR (toluene-d₈, 500 MHz, 295 K): δ ≈ 12.4 (br, fwhm = 670 Hz, 5H, Cp), 5.7 (br, fwhm = 225 Hz, 6H, Cy CH₂), 4.4 (br, fwhm ≈ 350 Hz, 6H, Cy CH₂), 3.0 (br, 12H, CH₂), 1.63 (br, fwhm = 30 Hz, 3H, Cy CH₂), 0.86 (br, fwhm = 55 Hz, 3H, Cy CH₂), -7.6 (br, fwhm ≈ 1500 Hz, 3H, Cy CH). No resonance observed in ³¹P{¹H} NMR spectrum, and ¹³C NMR spectrum was not recorded. A crystalline sample of higher analytical purity was obtained by dissolving 20 mg of the material in 0.6 mL of boiling MeCN in an NMR tube. The solution was left to stand at room temperature for several hours, affording about 15 mg of orange crystals, some of which were suitable for X-ray diffraction. Anal. Calcd. for C₂₅H₃₈O₂PCr: C, 66.21; H, 8.45. Found: C, 65.52; H, 8.22 (powder). Found: C, 65.91; H, 8.48 (crystals).

Synthesis of K⁺(18-crown-6)[CpCr(CO)₂(Ime)]⁻·0.5 THF. CpCr(CO)₂(Ime)[•] (0.071 g, 0.26 mmol) and an excess of K₈ (0.072 g, ≈ 0.5 mmol K) were stirred in 2 mL of THF, giving an orange solution (containing suspended graphite/KC₈ particles). After 30 min, the solution was filtered and added to a solution of 18-crown-6 (0.086 g, 0.33 mmol) in 1 mL of THF. Hexane (2 mL) was added, resulting in a slight cloudiness of the orange solution. The inside of the vial was scratched with a spatula, immediately inducing the precipitation of the title compound as thin, orange plates. The crystals were washed with Et₂O (3 × 2 mL) and dried under vacuum. Yield: 0.140 g (0.23 mmol, 87%). ¹H NMR (CD₃CN, 500 MHz, 293 K): δ 6.84 (s, 2H, =CH), 4.00 (s, 5H, Cp), 3.84 (s, 6H, N-CH₃), 3.64 (m, 2H, THF), 3.57 (s, 24H, 18-crown-6), 1.80 (m, 2H, THF). ¹³C{¹H} NMR (CD₃CN, 125 MHz, 293 K): δ 254.5 (s, Cr-CO), 223.3 (s, Cr-CN₂), 121.1 (s, =CH), 81.6 (s, Cp), 70.8 (s, 18-crown-6), 68.2 (s, THF), 39.2 (s, N-CH₃), 26.2 (s, THF). Anal. Calcd. for C₂₆H₄₁CrKN₂O_{8.5}: C, 51.30; H, 6.79; N, 4.60. Found: C, 49.78; H, 6.78; N, 4.54. Single crystals of K⁺(18-crown-6)[CpCr(CO)₂(Ime)]⁻·1/2 THF were grown by dissolving 12 mg of the material in 0.5 mL of boiling THF in an NMR tube. The solution was left to stand at room temperature for several hours, affording orange blocks.

Synthesis of K⁺[CpCr(CO)₂(Ime)]⁻ (crown-free). A solution of K⁺[CpCr(CO)₂(Ime)]⁻ was generated as described above. Addition of several volumes of hexane resulted in the precipitation of a yellow/orange powder. The powder was washed with Et₂O (3 × 4 mL) and dried, and K⁺[CpCr(CO)₂(Ime)]⁻ could be isolated in about 90% yield. The powder is very fluffy and is not convenient to handle. It was analyzed by IR spectroscopy, but not by elemental analysis. Single crystals of K⁺[CpCr(CO)₂(Ime)]⁻·3/4 THF were grown by dissolving 20 mg of the material in 0.5 mL of hot THF in an NMR tube (not all material dissolved). The solution was allowed to slowly concentrate over several weeks in the glovebox, affording orange blocks.

Table 4. Crystallographic Data

complex	$\text{CpCr}(\text{CO})_2(\text{IME})^{\bullet}$	$\text{K}^+(18\text{-crown-6})[\text{CpCr}(\text{CO})_2(\text{IME})]^{-}\cdot\frac{1}{2}\text{THF}$	$\text{K}^+[\text{CpCr}(\text{CO})_2(\text{IME})]^{-}\cdot\frac{3}{4}\text{THF}$	$\text{CpCr}(\text{CO})_2(\text{PCy}_3)^{\bullet}$	$\text{CpCr}(\text{CO})_2(\text{PCy}_3)\text{H}$
empirical formula	$\text{C}_{12}\text{H}_{13}\text{N}_2\text{O}_2\text{Cr}$	$\text{C}_{26}\text{H}_{41}\text{KN}_2\text{O}_{8.5}\text{Cr}$	$\text{C}_{15}\text{H}_{19}\text{KN}_2\text{O}_{2.75}\text{Cr}$	$\text{C}_{25}\text{H}_{38}\text{O}_2\text{PCr}$	$\text{C}_{25}\text{H}_{39}\text{O}_2\text{PCr}$
formula weight (g mol ⁻¹)	269.24	608.71	362.42	453.52	454.53
space group	$P\bar{1}$ (No. 2)	$Pca2_1$ (No. 29)	$P2_1$ (No. 4)	$P2_1/n$ (No. 14)	$P\bar{1}$ (No. 2)
unit cell lengths (Å)	<i>a</i> : 11.4850(5)	<i>a</i> : 16.4326(5)	<i>a</i> : 7.5173(2)	<i>a</i> : 14.5523(6)	<i>a</i> : 9.7528(5)
	<i>b</i> : 14.6464(7)	<i>b</i> : 22.3721(6)	<i>b</i> : 25.0725(6)	<i>b</i> : 10.0674(5)	<i>b</i> : 11.2597(7)
	<i>c</i> : 15.3720(7)	<i>c</i> : 16.2384(5)	<i>c</i> : 17.4342(4)	<i>c</i> : 15.7122(6)	<i>c</i> : 11.5526(7)
unit cell angles (deg)	α : 70.022(2)	α : 90	α : 90	α : 90	α : 74.059(3)
	β : 87.357(2)	β : 90	β : 98.219(2)	β : 94.732(3)	β : 73.138(3)
	γ : 87.104(2)	γ : 90	γ : 90	γ : 90	γ : 77.070(2)
volume (Å ³)	2425.93(19)	5969.8(3)	3252.20(14)	2294.05(17)	1153.00(12)
Z (Z')	8 (4)	8 (2)	8 (4)	4 (1)	2 (1)
calcd. density (g cm ⁻³)	1.474	1.355	1.480	1.313	1.309
μ (Mo K α , mm ⁻¹)	0.933	0.572	0.970	0.587	0.584
R1 ($I > 2\sigma(I)$) ^a	0.0869	0.0340	0.0389	0.0460	0.0387
wR2 (all data) ^b	0.2426	0.0791	0.0949	0.1213	0.1253

$$^a\text{R1} = (\sum \|F_o\| - |F_c|) / \sum |F_o|. \quad ^b\text{wR2} = [\sum w(F_o^2 - F_c^2)^2 / \sum w(F_o^2)^2]^{1/2}.$$

Synthesis of $\text{K}^+(18\text{-crown-6})[\text{CpCr}(\text{CO})_2(\text{PCy}_3)]^-$. $\text{CpCr}(\text{CO})_2(\text{PCy}_3)^{\bullet}$ (0.101 g, 0.223 mmol) was dissolved in THF (2 mL), and an excess of KCl (0.050 g, \approx 0.4 mmol K) was added. The suspension was stirred for 30 min, filtered, and added to a solution of 18-crown-6 (0.070 g, 0.26 mmol) in 0.5 mL of THF. Because some of the $\text{K}^+[\text{CpCr}(\text{CO})_2(\text{PCy}_3)]^-$ had precipitated, the black filter cake was washed with MeCN (ca. 5 mL total) until the initially yellow washings were nearly colorless. The resulting yellow MeCN/THF solution was evaporated to dryness, leaving a yellow powder, which was washed with hexane (4 \times 5 mL) and dried under vacuum. Yield: 0.150 g (0.198 mmol, 89%). ¹H NMR (CD_3CN , 500 MHz, 298 K): δ 4.06 (d, ³J_{HP} = 1.4 Hz, 5H, Cp), 3.58 (s, 24H, 18-crown-6), 2.02 (app d, 6H, Cy CH₂), 1.72 (m, 6H, Cy CH₂), 1.67 (m, 3H, Cy CH, overlapped), 1.64 (m, 3H, Cy CH₂, overlapped), 1.35 (app q, 6H, Cy CH₂), 1.19 (m, 6H, Cy CH₂, overlapped), 1.18 (m, 3H, Cy CH₂, overlapped). ¹³C{¹H} NMR (CD_3CN , 125 MHz, 298 K): δ 256.2 (d, ²J_{CP} = 18 Hz, Cr-CO), 80.6 (s, Cp), 70.9 (s, 18-crown-6), 41.5 (d, ¹J_{CP} = 9 Hz, Cy CH), 31.2 (d, ¹J_{CP} = 1 Hz, Cy CH₂), 29.1 (d, ¹J_{CP} = 9 Hz, Cy CH₂), 28.0 (d, ¹J_{CP} = 1 Hz, Cy CH₂). ³¹P{¹H} NMR (CD_3CN , 202 MHz, 298 K): δ 104.4 (s). Anal. Calcd. for $\text{C}_{37}\text{H}_{62}\text{KO}_8\text{PCr}$: C, 58.71; H, 8.26. Found: C, 55.97; H, 7.96.

Generation and Spectroscopic Characterization of $\text{CpCr}(\text{CO})_2(\text{IME})\text{H}$. An orange solution of $\text{K}^+(18\text{-crown-6})[\text{CpCr}(\text{CO})_2(\text{IME})]^{-}\cdot 0.5$ THF (16 mg, 26 μmol) in 0.3 mL of CD_3CN was combined with a colorless solution of $[\text{H-DBU}]^+\text{BF}_4^-$ (9 mg, 38 μmol , about 1.5 equiv) in 0.3 mL of CD_3CN , affording a light yellow solution. ¹H NMR (CD_3CN , 500 MHz, 293 K): δ 7.09 (s, 2H, =CH), 4.63 (s, 5H, Cp), 3.78 (s, 6H, N-CH₃), -5.33 (s, 1H, Cr-H). ¹³C{¹H} NMR (CD_3CN , 125 MHz, 293 K): δ 244.0 (s, Cr-CO), 198.8 (s, Cr-CN₂), 124.4 (s, =CH), 86.9 (s, Cp), 40.0 (br, N-CH₃).

Attempted Synthesis of $\text{CpCr}(\text{CO})_2(\text{IME})\text{H}$. $\text{K}^+(18\text{-crown-6})[\text{CpCr}(\text{CO})_2(\text{IME})]^{-}\cdot 0.5$ THF (51 mg, 84 μmol) and $\text{NH}_4^+\text{PF}_6^-$ (22 mg, 0.13 mmol) were suspended in a mixture of Et₂O (2.5 mL) and THF (0.5 mL). The mixture was stirred for about 15 min, until the orange crystalline starting material had reacted away, and a yellow solution of $\text{CpCr}(\text{CO})_2(\text{IME})\text{H}$ (containing a white precipitate) was obtained. The solution was filtered, and the volatiles were removed under vacuum. An orange, sticky residue was obtained; scraping resulted in solidification. IR analysis revealed that > 80% of [Cr] was in the form of $\text{CpCr}(\text{CO})_2(\text{IME})^{\bullet}$. On the basis of that result, attempts to purify this material were not undertaken.

Synthesis of $\text{CpCr}(\text{CO})_2(\text{PCy}_3)\text{H}$. A solution of $\text{K}^+(18\text{-crown-6})[\text{CpCr}(\text{CO})_2(\text{PCy}_3)]^-$ (0.101 g, 0.133 mmol) in MeCN (2 mL) was added to a solution of $\text{NH}_4^+\text{PF}_6^-$ (0.027 g, 0.17 mmol) in MeCN (1 mL). The color changed from orange to light yellow, and the product started to precipitate as a yellow crystalline material soon after combination of the reagents. The mixture was kept at -35 °C for 2h, after which the crystals were collected, washed with cold MeCN (4 \times 2 mL) and dried under vacuum. Yield: 0.049 g (0.11 mmol, \approx 80%). ¹H NMR (CD_3CN , 500 MHz, 298 K): δ 4.73 (d, ³J_{HP} = 0.8 Hz, 5H, Cp), 1.91 (m, 6H, Cy CH₂), 1.88 (m, 3H, Cy CH, overlapped), 1.82 (m, 6H, Cy CH₂), 1.69 (m, 3H, Cy CH₂), 1.40–1.19 (several m, 15H, Cy CH₂), -6.22 (d, ²J_{HP} = 80 Hz, 1H, Cr-H). ¹³C{¹H} NMR (CD_3CN , 125 MHz, 298 K): δ 86.1 (s, Cp), 40.7 (d, ¹J_{CP} = 18 Hz, Cy CH), 30.9 (d, ¹J_{CP} = 1.5 Hz, Cy CH₂), 28.5 (d, ¹J_{CP} = 10 Hz, Cy CH₂), 27.2 (d, ¹J_{CP} = 1 Hz, Cy CH₂). Because of low solubility, carbonyl carbons were not observed, even with 10,000 transients. ³¹P{¹H} NMR (CD_3CN , 202 MHz, 298 K): δ 91.2 (s). Anal. Calcd. for $\text{C}_{25}\text{H}_{39}\text{O}_2\text{PCr}$: C, 66.06; H, 8.65. Found: C, 65.78; H, 8.47. Single crystals of $\text{CpCr}(\text{CO})_2(\text{PCy}_3)\text{H}$ were grown by dissolving 9 mg of the material in 0.5 mL of boiling MeCN in an NMR tube. The solution was kept at 25 °C overnight, affording light yellow blocks.

Crystallography. For all reported structures, a 10 \times microscope was used to identify suitable crystals of the same habit. Each crystal was coated in Paratone, affixed to a Nylon loop, and placed under streaming nitrogen (100 K for the IME complexes, 145 K for the PCy₃ complexes) in a Bruker KAPPA APEX II CCD diffractometer with 0.71073 Å Mo K α radiation. The space groups were determined on the basis of systematic absences and intensity statistics. The structures were solved by direct methods and refined by full-matrix least-squares on *F*². Anisotropic displacement parameters were determined for all nonhydrogen atoms. Hydrogen atoms were placed at idealized positions and refined with fixed isotropic displacement parameters, with the exception of the Cr-bonded hydrogen in $\text{CpCr}(\text{CO})_2(\text{PCy}_3)\text{H}$, which was isotropically refined.

The structure of $\text{CpCr}(\text{CO})_2(\text{IME})^{\bullet}$ is of only moderate quality (*w*R2 = 0.24), and several significant peaks of residual electron density (ca. 2–3 e Å⁻³) were located within 1–2 Å of some of the Cr centers. These peaks were chemically meaningless. It is plausible that there is positional disorder in some of the molecules, but we have not been able to model this disorder. Refinement of $\text{K}^+(18\text{-crown-6})[\text{CpCr}(\text{CO})_2(\text{IME})]^{-}\cdot\frac{1}{2}\text{THF}$ (*Pca*2₁) gave a Flack parameter⁵⁶ of 0.226(9) (based on 9227 Friedel pairs, 95% of data), which we interpreted as an

indication for inversion twinning. Indeed, inclusion of twinning in the model refined to a fraction of 0.23(1) for the inverted structure. The refinement of $K^+[CpCr(CO)_2(Ime)]^{-3/4} \cdot THF$ ($P2_1$) gave a Flack parameter of 0.004(12) (based on 7135 Friedel pairs, 94% of data), which we interpret as an indication that the correct absolute structure was determined and that inclusion of inversion twinning was not required.

The following is a list of programs used: data reductions, SAINT-Plus version 6.63;⁵⁷ absorption correction, SADABS;⁵⁸ structural solutions, SHELXS-97;⁵⁹ structural refinement, SHELXL-97;⁶⁰ graphics, Ortep-3 (version 2.02)⁶¹ for Windows. Solution and refinement were done in the program OLEX2.⁶² Crystallographic data are listed in Table 4; electronic files (CIF format) are provided in the Supporting Information, and have also been deposited at the Cambridge Crystallographic Data Centre (CCDC 910168–910172).

■ ASSOCIATED CONTENT

■ Supporting Information

Additional details (tables, figure) on the reported crystal structures; ¹H NMR, IR, EPR, CV characterization data (figures); EPR spectra of $CpCr(CO)_2(PCy_3)^+$ and simulation details; crystallographic data (CIF format). This material is available free of charge via the Internet at <http://pubs.acs.org>.

■ AUTHOR INFORMATION

■ Corresponding Author

*E-mail: morris.bullock@pnnl.gov.

■ Notes

The authors declare no competing financial interest.

■ ACKNOWLEDGMENTS

We thank the U.S. Department of Energy, Office of Science, Office of Basic Energy Sciences, Division of Chemical Sciences, Geosciences and Biosciences for support. M.L.H. carried out the crystallographic studies and was supported as part of the Center for Molecular Electrocatalysis, an Energy Frontier Research Center funded by the U.S. Department of Energy, Office of Science, Office of Basic Energy Sciences. We thank Dr. John C. Linehan for assistance with the high-pressure NMR experiments, and Dr. Birgit Schwenzer for assistance with recording the NIR spectra. The EPR studies were performed at the William R. Wiley Environmental Molecular Sciences Laboratory (EMSL), a national scientific user facility sponsored by the Department of Energy's Office of Biological and Environmental Research located at PNNL. Pacific Northwest National Laboratory is operated by Battelle for the U.S. Department of Energy.

■ REFERENCES

- (1) Baird, M. C. *Chem. Rev.* **1988**, *88*, 1217–1227.
- (2) Scott, S. L.; Espenson, J. H.; Zhu, Z. *J. Am. Chem. Soc.* **1993**, *115*, 1789–1797.
- (3) Tyler, D. R. *Acc. Chem. Res.* **1991**, *24*, 325–331.
- (4) Cahoon, J. F.; Kling, M. F.; Sawyer, K. R.; Frei, H.; Harris, C. B. *J. Am. Chem. Soc.* **2006**, *128*, 3152–3153.
- (5) (a) Cahoon, J. F.; Kling, M. F.; Sawyer, K. R.; Andersen, L. K.; Harris, C. B. *J. Mol. Struct.* **2008**, *890*, 328–338. (b) Cahoon, J. F.; Kling, M. F.; Schmatz, S.; Harris, C. B. *J. Am. Chem. Soc.* **2005**, *127*, 12555–12565.
- (6) Zhang, J.; Grills, D. C.; Huang, K. W.; Fujita, E.; Bullock, R. M. *J. Am. Chem. Soc.* **2005**, *127*, 15684–15685.
- (7) (a) Eisenberg, D. C.; Lawrie, C. J. C.; Moody, A. E.; Norton, J. R. *J. Am. Chem. Soc.* **1991**, *113*, 4888–4895. (b) Eisenberg, D. C.; Norton, J. R. *Isr. J. Chem.* **1991**, *31*, 55–66.

- (8) (a) Hartung, J.; Pulling, M. E.; Smith, D. M.; Yang, D. X.; Norton, J. R. *Tetrahedron* **2008**, *64*, 11822–11830. (b) Choi, J.; Tang, L. H.; Norton, J. R. *J. Am. Chem. Soc.* **2007**, *129*, 234–240. (c) Tang, L. H.; Norton, J. R. *Macromolecules* **2006**, *39*, 8236–8240. (d) Tang, L. H.; Norton, J. R. *Macromolecules* **2006**, *39*, 8229–8235. (e) Tang, L. H.; Norton, J. R. *Macromolecules* **2004**, *37*, 241–243. (f) Tang, L. H.; Norton, J. R.; Edwards, J. C. *Macromolecules* **2003**, *36*, 9716–9720. (g) O'Connor, J. M.; Friese, S. J. *Organometallics* **2008**, *27*, 4280–4281.

- (9) Choi, J.; Pulling, M. E.; Smith, D. M.; Norton, J. R. *J. Am. Chem. Soc.* **2008**, *130*, 4250–4252.

- (10) Roberts, J. A. S.; Franz, J. A.; van der Eide, E. F.; Walter, E. D.; Petersen, J. L.; DuBois, D. L.; Bullock, R. M. *J. Am. Chem. Soc.* **2011**, *133*, 14593–14603.

- (11) Roberts, J. A. S.; Appel, A. M.; DuBois, D. L.; Bullock, R. M. *J. Am. Chem. Soc.* **2011**, *133*, 14604–14613.

- (12) van der Eide, E. F.; Liu, T. B.; Camaioni, D. M.; Walter, E. D.; Bullock, R. M. *Organometallics* **2012**, *31*, 1775–1789.

- (13) Tilset, M.; Parker, V. D. *J. Am. Chem. Soc.* **1989**, *111*, 6711–6717; as modified in *J. Am. Chem. Soc.* **1990**, *112*, 2843.

- (14) Kiss, G.; Zhang, K.; Mukerjee, S. L.; Hoff, C. D.; Roper, G. C. *J. Am. Chem. Soc.* **1990**, *112*, 5657–5658.

- (15) It is convenient to generate this carbene in solution (by the reaction of 1,3-dimethylimidazolium iodide with potassium hydride); the neat material has been reported to be much less stable than solutions of it. Arduengo, A. J., III; Dias, H. V. R.; Harlow, R. L.; Kline, M. *J. Am. Chem. Soc.* **1992**, *114*, 5530–5534.

- (16) Air exposure of $CpCr(CO)_2(Ime)^+$ solutions gives black, insoluble precipitates, which were not further characterized.

- (17) Atwood, C. G.; Geiger, W. E. *J. Am. Chem. Soc.* **1994**, *116*, 10849–10850.

- (18) Bertini, I.; Luchinat, C.; Parigi, G. *Solution NMR of Paramagnetic Molecules*. In *Current Methods in Inorganic Chemistry*; Elsevier: New York, 2001; Vol. 2, p 33.

- (19) (a) Wallen, S. L.; Schoenbachler, L. K.; Dawson, E. D.; Blatchford, M. A. *Anal. Chem.* **2000**, *72*, 4230–4234. (b) Yonker, C. R.; Linehan, J. C. *J. Organomet. Chem.* **2002**, *650*, 249–257.

- (20) (a) Hanaya, M.; Iwaizumi, M. *J. Organomet. Chem.* **1992**, *435*, 337–345. (b) Hanaya, M.; Iwaizumi, M. *Organometallics* **1989**, *8*, 672–676.

- (21) Connelly, N. G.; Geiger, W. E. *Chem. Rev.* **1996**, *96*, 877–910.

- (22) We classify the $K \cdots O \equiv C$ interaction as side-on when $\angle(K-O-C) \leq 90^\circ$ (an arbitrary cutoff). In those cases, dotted lines between potassium and the carbonyl carbons are drawn.

- (23) (a) The use of MeCN solvent for reductions using KC_8 may seem unusual (THF is more commonly used), but it has precedent (ref 23b). However, it is known that MeCN can be deprotonated by KC_8 (ref 23c), and we do not know whether the reduction of the radical occurs directly by KC_8 or by the cyanomethyl anion. (b) Mock, M. T.; Potter, R. G.; O'Hagan, M. J.; Camaioni, D. M.; Dougherty, W. G.; Kassel, W. S.; DuBois, D. L. *Inorg. Chem.* **2011**, *50*, 11914–11928. (c) Savoia, D.; Trombini, C.; Umani-Ronchi, A. *Tetrahedron Lett.* **1977**, *18*, 653–656.

- (24) Kaljurand, I.; Kütt, A.; Sooväli, L.; Rodima, T.; Mäemets, V.; Leito, I.; Koppel, I. A. *J. Org. Chem.* **2005**, *70*, 1019–1028.

- (25) Coetzee, J. F.; Padmanabhan, G. R. *J. Am. Chem. Soc.* **1965**, *87*, 5005–5010.

- (26) We found (ref 12) that $CpW(CO)_2(Ime)H$ exists in solution as a mixture of cis and trans isomers; they interconvert slow enough to be distinguished by ¹H NMR spectroscopy. Cis/trans isomerism may occur for $CpCr(CO)_2(Ime)H$ as well, but only one set of ¹H NMR signals is observed.

- (27) Schwesinger, R.; Willaredt, J.; Schlemper, H.; Keller, M.; Schmitt, D.; Fritz, H. *Chem. Ber.* **1994**, *127*, 2435–2454.

- (28) Tolman, C. A. *Chem. Rev.* **1977**, *77*, 313–348.

- (29) Cheng, T.-Y.; Brunshwig, B. S.; Bullock, R. M. *J. Am. Chem. Soc.* **1998**, *120*, 13121–13137.

- (30) (a) Crabtree, R. H. *The Organometallic Chemistry of the Transition Metals*, 5th ed.; Wiley: New York, 2009; p 76. (b) Bau, R.;

Teller, R. G.; Kirtley, S. W.; Koetzle, T. F. *Acc. Chem. Res.* **1979**, *12*, 176–183.

(31) Wayner, D. D. M.; Parker, V. D. *Acc. Chem. Res.* **1993**, *26*, 287–294.

(32) Ellis, W. W.; Raebiger, J. W.; Curtis, C. J.; Bruno, J. W.; DuBois, D. L. *J. Am. Chem. Soc.* **2004**, *126*, 2738–2743.

(33) The hydricity (ΔG_{H^+}) of $\text{CpCr}(\text{CO})_2(\text{IME})\text{H}$ (59.2(9) kcal mol⁻¹) was also determined, using the equation $\Delta G_{\text{H}^+}(\text{MH}) = 1.37 \text{ p}K_{\text{a}}(\text{MH}) + 23.06 [E^\circ(\text{M}^{+/-}) + E^\circ(\text{M}^{+/\bullet})] + 79.6$. Note that we use $E^\circ(\text{MS}^+/\text{M}^{\bullet})$ instead of $E^\circ(\text{M}^{+/\bullet})$, so that coordination of MeCN to the 16-electron cation M^+ (to form MS^+) is taken into account. We conservatively assign a relatively large uncertainty of ± 30 mV to $E^\circ(\text{MS}^+/\text{M}^{\bullet})$; the wave is quasi-reversible, and E° may slightly deviate from $E_{1/2}$. The hydricity of $\text{CpCr}(\text{CO})_2(\text{IME})\text{H}$ is similar to the 57(1) kcal mol⁻¹ (ref 11) for the tungsten complex $\text{CpW}(\text{CO})_2(\text{IMes})\text{H}$ (IMes = 1,3-dimesitylimidazol-2-ylidene), also taking the formation of MS^+ into account.

(34) Watkins, W. C.; Hensel, K.; Fortier, S.; Macartney, D. H.; Baird, M. C.; McLain, S. J. *Organometallics* **1992**, *11*, 2418–2424.

(35) Cooley, N. A.; Watson, K. A.; Fortier, S.; Baird, M. C. *Organometallics* **1986**, *5*, 2563–2565.

(36) Fortier, S.; Baird, M. C.; Preston, K. F.; Morton, J. R.; Ziegler, T.; Jaeger, T. J.; Watkins, W. C.; MacNeil, J. H.; Watson, K. A.; Hensel, K.; Le Page, Y.; Charland, J.-P.; Williams, A. J. *J. Am. Chem. Soc.* **1991**, *113*, 542–551.

(37) (a) Ackermann, K.; Hofmann, P.; Köhler, F. H.; Kratzer, H.; Krist, H.; Öfele, K.; Schmidt, H. R. *Z. Naturforsch. B* **1983**, *38*, 1313–1324. (b) Öfele, K. *J. Organomet. Chem.* **1968**, *12*, P42–P43. (c) Tafipolsky, M.; Scherer, W.; Öfele, K.; Artus, G.; Pedersen, B.; Herrmann, W. A.; McGrady, G. S. *J. Am. Chem. Soc.* **2002**, *124*, 5865–5880.

(38) (a) Adams, R. D.; Collins, D. E.; Cotton, F. A. *J. Am. Chem. Soc.* **1974**, *96*, 749–754. (b) McLain, S. J. *J. Am. Chem. Soc.* **1988**, *110*, 643–644.

(39) (a) A CSD search (version 5.33, August 2012) for 5-membered NHC complexes of chromium gave 37 hits. (b) Cr–C_(carbene) bond lengths in other Cr-IME complexes: $\text{Cr}(\text{CO})_4(\text{IME})_2$, 2.131(3) Å (ref 37a.); $[\text{Cr}(\text{CO})_4(\text{IME})_2]^+[\text{PF}_6]^-$, 2.113(4) and 2.119(4) Å (ref 37a.); $\text{Cr}(\text{CO})_5(\text{IME})$, 2.138(2) and 2.145(2) Å (two independent molecules, ref 37c.). (c) For a monodentate NHC, the heretofore shortest Cr–C_(carbene) bond length is 2.075(4) Å, found in (benzimidazol-2-ylidene)Cr(CO)₅. See: Hahn, F. E.; Langenhahn, V.; Meier, N.; Lügger, T.; Fehlhammer, W. P. *Chem.—Eur. J.* **2003**, *9*, 704–712.

(40) Hammack, D. J.; Dillard, M. M.; Castellani, M. P.; Rheingold, A. L.; Rieger, A. L.; Rieger, P. H. *Organometallics* **1996**, *15*, 4791–4797.

(41) Rieger, P. H. *Coord. Chem. Rev.* **1994**, *135/136*, 203–286.

(42) Woska, D. C.; Ni, Y. P.; Wayland, B. B. *Inorg. Chem.* **1999**, *38*, 4135–4138.

(43) Tilset, M. *J. Am. Chem. Soc.* **1992**, *114*, 2740–2741.

(44) Fischer, P. J.; Heerboth, A. P.; Herm, Z. R.; Kucera, B. E. *Organometallics* **2007**, *26*, 6669–6673.

(45) Hey-Hawkins, E.; von Schnering, H. G. *Z. Naturforsch. B* **1991**, *46*, 621–624.

(46) Braunschweig, H.; Radacki, K.; Kraft, K.; Stellwag, S. *Z. Naturforsch. B* **2010**, *65*, 1073–1076.

(47) (a) Darensbourg, M. Y. *Prog. Inorg. Chem.* **1985**, *33*, 221–274.

(b) Darensbourg, M. Y.; Jimenez, P.; Sackett, J. R.; Hanckel, J. M.; Kump, R. L. *J. Am. Chem. Soc.* **1982**, *104*, 1521–1530.

(48) Moore, E. J.; Sullivan, J. M.; Norton, J. R. *J. Am. Chem. Soc.* **1986**, *108*, 2257–2263.

(49) Parker, V. D.; Handoo, K. L.; Roness, F.; Tilset, M. *J. Am. Chem. Soc.* **1991**, *113*, 7493–7498.

(50) Burchell, R. P. L.; Sirsch, P.; Decken, A.; McGrady, G. S. *Dalton Trans.* **2009**, 5851–5857.

(51) Skagestad, V.; Tilset, M. *J. Am. Chem. Soc.* **1993**, *115*, 5077–5083.

(52) (a) The low stability of $\text{CpCr}(\text{CO})_2(\text{IME})(\text{MeCN})^+$ and the quasi-reversible electrochemical oxidation of $\text{CpCr}(\text{CO})_2(\text{IME})^{\bullet}$ in

MeCN may be explained in the same way, as steric pressure could facilitate the (reversible) dissociation of MeCN. Even if only small equilibrium quantities of 16-electron $\text{CpCr}(\text{CO})_2(\text{IME})^+$ are present in MeCN solution, this would provide a pathway for decomposition and for the electrochemical reduction of $\text{CpCr}(\text{CO})_2(\text{IME})(\text{MeCN})^+$ to $\text{CpCr}(\text{CO})_2(\text{IME})^{\bullet}$ by a CE mechanism. Little is known about related cations. However, the tricarbonyl $\text{CpCr}(\text{CO})_3(\text{MeCN})^+$ has been isolated as the PF_6^- salt (ref 52b), its electrochemistry in MeCN is known (ref 52c), and it has been reported to be unstable in CH_2Cl_2 (ref 52d). (b) Herberhold, M.; Ott, J.; Haumaier, L. *Chem. Ber.* **1985**, *118*, 3143–3150. (c) Tilset, M. *Inorg. Chem.* **1994**, *33*, 3121–3126. (d) Ryan, O. B.; Tilset, M.; Parker, V. D. *J. Am. Chem. Soc.* **1990**, *112*, 2618–2626.

(53) Birdwhistell, R.; Hackett, P.; Manning, A. R. *J. Organomet. Chem.* **1978**, *157*, 239–241.

(54) Benac, B. L.; Burgess, E. M.; Arduengo, A. J., III *Org. Synth.* **1986**, *64*, 92–95.

(55) Stoll, S.; Schweiger, A. *J. Magn. Reson.* **2006**, *178*, 42–55.

(56) (a) Flack, H. D.; Bernardinelli, G. *Acta Crystallogr., Sect. A* **1999**, *55*, 908–915. (b) Flack, H. D.; Bernardinelli, G. *J. Appl. Crystallogr.* **2000**, *33*, 1143–1148.

(57) SAINT, v. 6.63; Bruker AXS Inc.: Madison, WI.

(58) Sheldrick, G. M. *SADABS Program for Absorption Correction of Area Detector Frames*; Bruker AXS.: Madison, WI.

(59) Sheldrick, G. M. *SHELXS-97 Program for Crystal Structure Solution*; Institut für Anorganische Chemie der Universität Göttingen: Göttingen, Germany, 1997.

(60) Sheldrick, G. M. *SHELXL-97 Program for Crystal Structure Refinement*; Institut für Anorganische Chemie der Universität Göttingen: Göttingen, Germany, 1997.

(61) Farrugia, L. J. *J. Appl. Crystallogr.* **1997**, *30*, 565.

(62) Dolomanov, O. V.; Bourhis, L. J.; Gildea, R. J.; Howard, J. A. K.; Puschmann, H. *J. Appl. Crystallogr.* **2009**, *42*, 339–341.